Reconstructing Generalized Exponential Laws by Self-Similar Exponential Approximants

S.Gluzman[1], D. Sornette[1,2,3] and V.I. Yukalov[4,5]

[1] *Institute of Geophysics and Planetary Physics*

University of California, Los Angeles, California 90095

[2] *Department of Earth and Space Science*

University of California, Los Angeles, California 90095

[3] *Laboratoire de Physique de la Matière Condensée*

CNRS UMR6622 and Université des Sciences

Parc Valrose, 06108 Nice Cedex 2, France

[4] *Research Center for Optics and Photonics*

Instituto de Fisica de São Carlos, Universidade de São Paulo

Caixa Postal 369, São Carlos, São Paulo 13560-970, Brazil

[5] *Bogolubov Laboratory of Theoretical Physics*

Joint Institute for Nuclear Research, Dubna 141980, Russia

Abstract

We apply the technique of self-similar exponential approximants based on successive truncations of continued exponentials to reconstruct functional laws of the quasi-exponential class from the knowledge of only a few terms of their power series. Comparison with the standard Padé approximants shows that, in general, the self-similar exponential approximants provide significantly better reconstructions.

I. INTRODUCTION

Exponential laws are ubiquitous in nature. The overwhelming majority of relaxation phenomena occur through exponential laws. The dominant role played by exponential laws results from a combination of mechanisms. First, exponential relaxations result from viscous dissipation proportional to the first-order time derivative of the dynamical quantity, which is usually the dominant term breaking the time-reversal symmetry (see however [1] for a case where the third-order derivative becomes important). Second, exponential decay or growth reflects the first-order expansion in the rate of change as a function of the observable. Third, exponential laws are often associated with the Poisson process, which has the unique property of being memoryless. This leads to a remarkable mathematical property: the Poisson law is invariant with respect to any conditioning on the past or future and can thus be seen as the unique fixed-point of arbitrary transformations of time distributions involving conditioning [2].

These universal properties provide useful benchmarks against which deviations can be gauged. These departures usually betray specific mechanisms at work in real systems, that are otherwise hidden by the just-mentioned universal mechanisms. This is why the study of such laws which are close to exponentials is so important. It may happen, however, that we are not able to observe in some experiment or to study theoretically such a law, say a relaxation process, from its beginning till its very end. In theoretical works, this repeatedly happens when considering complicated problems that do not allow for exact solutions. Then, invoking some kind of perturbation theory, one may calculate a few successive approximations. The standard situation is when one employs a short-time expansion resulting in approximations presented as polynomials over time. The main problem in such cases is how to reconstruct the overall process from the knowledge of only its short-time behavior represented by a series in powers of time. An analogous situation may also arise in experiments, when one cannot, because of some technical difficulties, continuously measure the whole temporal process, but one is able to gain information only from a limited number of

measurements performed at discrete times. In that case again, one often presents the results in the simplest form of a polynomial describing the given set of discrete points.

It may also happen that the whole relaxation process is impossible to observe experimentally because the lifetime of a system is shorter than the relaxation time of the process being studied. For instance, intensive investigations of various physical processes are now being accomplished for trapped atoms (see reviews [3]- [5]). Since the life time of atoms in a trap is finite, not all processes can be observed in full, in particular phenomena associated with trapped spinor Bose condensates [6,7].

One more example of the same problem arises when the characteristic relaxation times are too long to allow for convenient experiments covering the full range of the relaxation. Let us mention the spin-lattice relaxation in polarized nuclear magnets [8,9], in which the relaxation time may attain several days at low temperatures. Another illustration is the magnetic relaxation in molecular magnets [10]- [12], where the relaxation time ranges up to several months below the blocking temperature. There are cases when the characteristic times become comparable to or larger than human time scales, as for instance in visco-elastic relaxation in the earth crust after earthquakes [13,14]. Here, seismologists may only observe the early part of the relaxation process which may last for decades to centuries. In general, if one extracts information only from the beginning of a process, the result can again be presented as a power series. And the question that arises is how to find the general relaxation law from the knowledge of only its short-term presentation.

Here, we suggest a technique to address this question of how to derive the whole sought function based on a perturbative expansion for short-time dynamics. To this end, we exploit the remarkable property of self-similar exponential approximants introduced in Ref. [15], which is able to reconstruct exactly the exponential function $\exp(-t)$ from the knowledge of only the two first terms of its Taylor expansion. In other words, the technique of self-similar exponential approximants represents an ideal filter for the exponential function. It is thus natural to expect that this technique can be successfully applied for the reconstruction of continuous functions deviating from a pure exponential while still keeping the same expo-

nential asymptotics at infinity, from the sole knowledge of their Taylor expansion for short times. We note that the self-similar exponential approximants generalize and give a systematic justification of the method of summation of power series by continued exponentials proposed by Bender and Vinson [16] as an alternative to Padé techniques, which themselves the result of truncated continued fraction representations of power series.

In the next section, we briefly review the main properties of the technique of self-similar exponential approximants that will be useful for our purpose. In section 3, we then discuss several examples illustrating its power to reconstruct quasi-exponential laws. In section 4, we apply the technique to an ordinary nonlinear differential equation motivated by a solid-friction problem. In each case, we compare our results with those from the more standard Padé approximants. In general, we find that the numerical errors of the reconstructions are significantly smaller for self-similar exponential approximants than for the standard Padé approximants.

II. SELF-SIMILAR EXPONENTIAL APPROXIMANTS

The complete mathematical foundation of the method can be found in Refs. [15], [17]-[21]. Here, we give a brief sketch which emphasizes the variant that is mostly appropriate for filtering exponential-type laws. Assume that we are interested in a function $\phi(t)$ of a real variable t. Let perturbation theory (or some fitting procedure) give for this function the perturbative approximations $\phi_n(t)$, with $n = 0, 1, 2, ...$ enumerating the approximation order. Consider the case when the perturbative procedure results in a polynomial

$$\phi_n(t) \simeq \sum_{k=0}^{n} a_k \; t^k \qquad (t \to 0), \qquad n = 0, 1, \ldots \tag{1}$$

Let us stress that the expansion (1) has, as a rule, no direct meaning if continued straightforwardly to the region of finite arbitrary t. In theoretical physics, the problem of reconstructing the value of a function at some distant moment of time from the knowledge of its asymptotic expansion as $t \to 0$, is called the renormalization or resummation problem. An analytical

tool for the solution of this problem, called algebraic self-similar renormalization, has been recently developed [15], [17]- [21]. The polynomial representation (1) gives for the sought function the following n polynomial approximations $p_i(t),\ i = 0, 2, ..., n$,

$$p_0(t) = a_0, \quad p_1(t) = a_0 + a_1 t, \quad p_2(t) = p_1(t) + a_2 t^2, \dots , \quad p_n(t) = p_{n-1}(t) + a_n t^n. \qquad (2)$$

The algebraic self-similar renormalization starts by applying to the approximations (2) an algebraic transformation, thus defining a new sequence, $P_i(t, s) = t^s p_i(t),\ i = 0, 2, ..., n$, with $s \geq 0$. This transformation raises the powers of the series (1), (2), and allows us to take effectively into consideration a longer timespan of the system history. We shall use below the strongest form of such transformation occurring by taking formally the limit $s \to \infty$. It can be shown that this results in an exponential representation of the sought function. The next step of the self-similar approximation theory [22]- [25] consists in considering the sequence of transformed approximations, $P_i(t, s)$, as a dynamical system in discrete time $i = 0, 1, ..., n$, that we call "time-order" to distinguish it from the time variable t. In order to define the system evolution in time-order, it is convenient to introduce a new variable φ and to define the so-called expansion function $t(\varphi, s)$ from the equation $P_0(t, s) = a_0 t^s = \varphi$, which gives $t(\varphi, s) = (\varphi/a_0)^{1/s}$. This makes it possible to construct the cascade of approximations $y_i(\varphi, s) \equiv P_i(\ t(\varphi, s), s)$. Embedding this cascade into a continuous approximation flow, one can write the evolution equation in terms of the discrete time-order variable in the form of the functional self-similarity relation, $y_{i+p}(\varphi, s) = y_i(y_p(\varphi, s), s)$, which is also the necessary condition for the convergence of P_i. Already at this stage, we can try to check the effectiveness of the algebraic transformation by calculating the so-called local multipliers,

$$m_i(t, s) \equiv \left[\frac{\partial y_i(\varphi.s)}{\partial \varphi} \right]_{\varphi = P_0(t,s)} , \qquad (3)$$

as $s \to \infty$. When all $|m_i(t, \infty)| < 1$, the convergence of the sequence P_i is guaranteed. To implement the calculations concretely, one can use the integral form of the self-similarity relation,

$$\int_{P_{i-1}}^{P_i^*} \frac{d\varphi}{v_i(\varphi, s)} = \tau,$$

where the cascade velocity is $v_i(\varphi, s) = y_i(\varphi, s) - y_{i-1}(\varphi, s)$ and τ is the minimal number of steps of the approximation procedure needed to reach the fixed point $P_i^*(t, s)$ of the approximation cascade. It is possible to find $P_i^*(t, s)$ explicitly and to perform an inverse algebraic transform after which the limit $s \to \infty$ is to be taken. The first step of the self-similar renormalization is completed. This procedure is then repeated as many times as necessary to renormalize all polynomials which appear at the preceding steps. Completing this program, we come to the following sequence of self-similar exponential approximations

$$p_j^*(t, \tau_1, \tau_2, ..., \tau_j) = a_0 \exp\left(\frac{a_1}{a_0}\tau_1 t \exp\left(\frac{a_2}{a_1}\tau_2 t ... \exp\left(\frac{a_j}{a_{j-1}}\tau_j t\right)\right)...\right), \quad j = 2, 3..., n. \tag{4}$$

The quantities $\tau_1,\ \tau_2, \ldots$ play the role of control functions that are to be defined from optimization conditions. For the purpose of reconstructing an exponential-type law, the optimal choice of controls τ_i is obtained by expanding $p_j^*(t, \tau_1, \tau_2, ..., \tau_j)$ in the vicinity of $t = 0$ and demanding that this expansion coincides with $\phi_j(t)$. In the theory of Padé approximants, this condition is often refered to as the "accuracy-through-order relationship." This method of determination of the control coefficients τ_i makes the self-similar exponential approximants analogous to the Euler superexponentials [16,26,27]. With this determination of the control parameters, we come finally to the self-similar approximants ϕ_j^* of the sought function,

$$\phi_j^*(t, \tau_1, \tau_2, \ldots, \tau_j) = p_j^*(t, \tau_1, \tau_2, \ldots, \tau_j) \; .$$

For example,

$$\phi_2^*(t, \tau_1, \tau_2) = a_0 \exp\left(\frac{a_1}{a_0}\tau_1 t \exp\left(\frac{a_2}{a_1}\tau_2 t\right)\right),$$

$$\phi_3^*(t, \tau_1, \tau_2, \tau_3) = a_0 \exp\left(\frac{a_1}{a_0}\tau_1 t \exp\left(\frac{a_2}{a_1}\tau_2 t \exp\left(\frac{a_3}{a_2}\tau_3 t\right)\right)\right),$$

$$\phi_4^*(t, \tau_1, \tau_2, \tau_3, \tau_4) = a_0 \exp\left(\frac{a_1}{a_0}\tau_1 t \exp\left(\frac{a_2}{a_1}\tau_2 t \exp\left(\frac{a_3}{a_2}\tau_3 t \exp\left(\frac{a_4}{a_3}\tau_4 t\right)\right)\right)\right).$$

In order to check whether the sequence of $\phi_j^*(t, \tau_1, \tau_2, ..., \tau_j)$ converges, we study their mapping multipliers, $M_j^*(t, \tau_1, \tau_2, \ldots \tau_j)$ defined as

$$M_j^*(t, \tau_1, \ldots, \tau_j) \equiv \frac{\delta \phi_j^*(t, \tau_1, \ldots, \tau_j)}{\delta p_1(t)} = \frac{1}{a_1} \frac{\partial}{\partial t} \phi_j^*(t, \tau_1, \ldots, \tau_j) \; . \tag{5}$$

This definition of the multipliers allows us to compare the convergence of the expansion and of the renormalized expressions, making clear what can be expected a priori.

With the control parameters defined as prescribed above for each j from the the accuracy-through-order relationship, we can obtain j self-similar exponential approximants for the sought function (where all τ are now known functions of the parameters a_i):

$$\phi^*_{j1}(t) = \phi^*_j(t, \tau_1, 1, ..., 1), \quad \phi^*_{j2}(t) = \phi^*_j(t, \tau_1, \tau_2, 1, ..., 1), \quad \phi^*_{jj}(t) = \phi^*_j(t, \tau_1, \tau_2, ..., \tau_j),$$

which differ according to the number of control parameters being employed. This provides a matrix of self-similar approximants, indexed by the order j and by the number of control parameters. To this matrix of approximants is associated the matrix of multipliers. E.g., for $j = 4$, we have

$$\phi^*_{21}(t) = \phi^*_j(t, \tau_1, 1), \qquad \phi^*_{22}(t) = \phi^*_j(t, \tau_1, \tau_2),$$

$$\phi^*_{31}(t) = \phi^*_3(t, \tau_1, 1, 1), \quad \phi^*_{32}(t) = \phi^*_3(t, \tau_1, \tau_2, 1), \quad \phi^*_{33}(t) = \phi^*_3(t, \tau_1, \tau_2, \tau_3),$$

$$\phi^*_{41}(t) = \phi^*_4(t, \tau_1, 1, 1, 1)\ , \qquad \phi^*_{42}(t) = \phi^*_4(t, \tau_1, \tau_2, 1, 1)\ ,$$

$$\phi^*_{43}(t) = \phi^*_4(t, \tau_1, \tau_2, \tau_3, 1)\ , \qquad \phi^*_{44}(t) = \phi^*_4(t, \tau_1, \tau_2, \tau_3, \tau_4).$$

We propose to qualify the convergence towards the sought function by examining both the convergence of the different sequences of multipliers M^* and of the approximants ϕ^*, choosing among them the pair which exhibits the best convergence rate. The resulting limiting point from the table of approximants should be taken for the value of the sought function. If there are more than one limiting point, one can take their weighted average, following Ref. [21].

III. ILLUSTRATION OF TECHNIQUE IN ACTION

We now present explicit examples demonstrating how the technique works.

A. Ideal Filter

Consider the Taylor expansion of the exponential function, $\phi(t) = \exp(-t)$, up to an arbitrary order in t,

$$\phi_n(t) \simeq \sum_{k=0}^{n} a_k \; t^k \; , \tag{6}$$

where

$$a_0 = 1, \quad a_1 = -1, \quad a_2 = \frac{1}{2}, \quad a_3 = -\frac{1}{6}, \quad a_4 = \frac{1}{24}, \quad a_5 = -\frac{1}{120}.$$

The second-order self-similar approximant is

$$\phi_{22}^*(t) = a_0 \exp\left(\frac{a_1}{a_0}\; t\; \tau_1 \exp\left(\frac{a_2}{a_1}\; t\; \tau_2\right)\right), \qquad \tau_1 = 1, \quad \tau_2 = 1 - \frac{1}{2}\,\frac{a_1^2}{a_2 a_0} = 0.$$

The fact that $\tau_2 = 0$ leads to $\phi_{22}^*(t) = \exp(-t)$. It also makes any arbitrary order approximant $\phi_{jj}^*(t)$ identical to $\exp(-t)$. Note, that all other approximants, except ϕ_{21}^*, ϕ_{31}^*, ϕ_{41}^* and ϕ_{51}^*, become identical to $\exp(-t)$ and all higher order control parameters are identical zeros, like τ_2.

Consider now the conventional Padé approximants, $\mathrm{P}_3^2(t)$ and $\mathrm{P}_4^1(t)$ ($\mathrm{P}_1^4(t)$ and $\mathrm{P}_2^3(t)$ have inferior quality) and compare them to the exact function, see Fig. 1. Although $\mathrm{P}_3^2(t)$ remains positive, it behaves nonmonotically. On the other hand, $\mathrm{P}_4^1(t)$ becomes negative for large t. These are typical problems encountered while attempting to reconstruct functions with exponential asymptotic behavior by means of Padé approximants. The relative percentage errors for those two Padé approximants are shown in Fig. 2. One should not be mislead by the seemingly superior performance of $\mathrm{P}_4^1(t)$, which is qualitatively wrong in predicting negative values already for moderate times. Because of this, we will present below only the relative percentage error for positively defined Padé approximants.

Let us study the impact of noise on the coefficients of the power law expansion (6). Since $\phi_{22}^*(t)$ recovers the exact solution in absence of noise, we study its perturbed value denoted $\phi_{22}^*(t, \eta, \theta)$ brought by the existence of the noises η and θ on the two first coefficients of the expansion (6) defined by the replacement of a_1 by $a_1(1+\eta)$ and/or of a_2 by $a_2(1+\theta)$. For sufficiently small amplitudes of the fluctuations, one can expand $\phi_{22}^*(t, \eta, \theta)$ as follows (only the most simple cases are considered):

$$\phi_{22}^*(t, \eta, 0) - \phi_{22}^*(t) \simeq b_1(t)\; \eta + b_2(t)\; \eta^2 + ...,$$

and

$$\phi^*_{22}(t,0,\theta) - \phi^*_{22}(t) \simeq c_1(t)\ \theta + c_2(t)\ \theta^2 + ...,$$

where all coefficients can be easily calculated analytically. We observe that:

1. the absolute error in the lowest order tends to peak at intermediate times, see Fig 3, while the relative error monotonously increases with time;

2. the absolute error caused by fluctuations in a_2 is smaller than the error caused by fluctuations of equivalent magnitude in a_1, see Fig 3;

3. higher order terms in the expansion tend to shift the peak in the absolute error towards larger times, see Fig. 4;

4. Interference of the error peaks at different orders leads to broaden the domain in time over which the errors are significant, see Fig. 4.

It is possible to perform an averaging over the random variables and evaluate the corresponding averages as a formal series to develop a specific resummation procedure that may provide a solution for the average function, even for arbitrary strong noises. We do not persue this here and return to the study of how self-similar exponential approximants, which are ideal filters for the exponential function, extract information on other functions which are perturbations of exponentials, from a few starting terms of their Taylor expansions.

B. Weak perturbation

Consider the function, $\phi(t) = \sin(t)^2 \exp(-t^2)$, which is nonmonotonic. Its expansion is

$$\phi_5(t) \simeq t^2 \sum_{k=0}^{5} a_k\ t^{2k}\ , \tag{7}$$

where

$$a_0 = 1, \quad a_1 = -\frac{4}{3}\ , \quad a_2 = \frac{79}{90}\ , \quad a_3 = -\frac{8}{21}\ , \quad a_4 = \frac{13921}{113400}\ , \quad a_5 = -\frac{29341}{935550}\ .$$

The coefficients alternate in sign, like in the ideal exponential example. The values of the control parameters,

$$\tau_2 = 0.013, \quad \tau_3 = -0.137, \quad \tau_4 = -0.131, \quad \tau_5 = -0.152,$$

are all negative, with τ_2 being rather small, which guarantees a good quality of the approximation already in the lowest nontrivial order. Higher-order approximants provide corrections to the good starting approximation $\phi^*_{22}(t)$.

Both multipliers and approximants converge extremely well. It is difficult to distinguish in Fig. 5 the approximant $\phi^*_{55}(t)$ from the exact function. The relative error at $t = 2$ is 0.045% for this approximant, while $\phi_5(t = 2)$ defined in (7) has a very large error -4.058×10^5 %. Note that the nondiagonal forms ϕ^*_{41} and ϕ^*_{51} approximate the sought function rather badly compared to the diagonal approximants. The logarithms of the relative percentage errors for the Padé approximant $\mathrm{P}^2_3(t)$ and for the super-exponential approximant $\phi^*_{55}(t)$, corresponding to the same number of terms used in the construction of both approximants, are shown in Fig. 6.

C. "Badly damaged" expansion

Let us consider a function with an expansion whose coefficients do not alternate in sign, such as $\phi(t) = \ln(1 + t) \exp(-t^2)$, which has the expansion

$$\phi_5(t) \simeq t \sum_{k=0}^{5} a_k \, t^k \; , \tag{8}$$

with the coefficients

$$a_0 = 1 \; , \quad a_1 = -\frac{1}{2} \; , \quad a_2 = -\frac{2}{3} \; , \quad a_3 = \frac{1}{4} \; , \quad a_4 = \frac{11}{30} \; , \quad a_5 = -\frac{1}{6} \; .$$

This is again a nonmonotonic function. The control parameters,

$$\tau_2 = 1.187, \quad \tau_3 = 1.69, \quad \tau_4 = -0.296, \quad \tau_5 = 0.661,$$

have different signs, with τ_2 and τ_3 being rather large, which leads to a poor quality of approximation to the exact function for $\phi^*_{22}(t)$ and $\phi^*_{33}(t)$. Rather than finding a good approximation to the exact solution already at the first step of the construction, the successive self-similar exponential approximants bracket the exact function within a rather broad range, as seen from the change of the sign between τ_3 and τ_4. The analysis of the multipliers shown

in Fig. 7 shows that $M_{44}^*(t)$ and $M_{55}^*(t)$ are the closest, which suggests a better convergence and that $\phi_{55}^*(t)$ and $\phi_{44}^*(t)$ are the two best approximants. Indeed, they are much closer to the exact function than the lower-order approximants as shown in Fig. 8. Also, since $|M_{55}^*(t)| < |M_{44}^*(t)|$, one can anticipate correctly that $\phi_{55}^*(t)$ is located closer to the exact solution than $\phi_{44}^*(t)$.

Consider all Padé approximants ($\mathrm{P}_3^2(t)$, $\mathrm{P}_4^1(t)$, $\mathrm{P}_1^4(t)$, and $\mathrm{P}_2^3(t)$) which can be built from the fifth-order polynomial (8). One can see in Fig. 9 that their quality is by far inferior to that obtained with ϕ_{55}^*. Fig. 10 shows the logarithm of the relative percentage errors for the self-similar exponential approximant $\phi_{55}^*(t)$ and for the Padé approximant $\mathrm{P}_1^4(t)$, which is the only one remaining positive.

D. Strong perturbation

Consider the Taylor expansion $\phi_5(t) \simeq \sum_{k=0}^5 a_k\ t^k$ of the exponential-type function, $\phi(t) = \frac{1}{1+t}\exp(-t)$, up to the fifth order in t, with the coefficients

$$a_0 = 1, \quad a_1 = -2, \quad a_2 = \frac{5}{2}, \quad a_3 = -\frac{8}{3}, \quad a_4 = \frac{65}{24}, \quad a_5 = -\frac{163}{60}.$$

The coefficients alternate in sign but their amplitudes behave nonmonotically. The approximants $\phi_{22}^*(t)$, $\phi_{33}^*(t)$, $\phi_{44}^*(t)$, $\phi_{55}^*(t)$, and multipliers $M_{22}^*(t)$, $M_{33}^*(t)$, $M_{44}^*(t)$, $M_{55}^*(t)$ for the sought function can be readily written down. The values of the control parameters,

$$\tau_2 = 0.2, \quad \tau_3 = 0.508, \quad \tau_4 = 0.377, \quad \tau_5 = 0.378,$$

are all positive and smaller than one.

Fig.11 shows the dependence of the multipliers as a function of time. One can observe that $M_{44}^*(t)$ and $M_{55}^*(t)$ are the closest pair, suggesting a good convergence of the cascade of approximants. The corresponding approximants, $\phi_{44}^*(t)$ and $\phi_{55}^*(t)$ bracket the exact function from above and below respectively, see Fig. 12. One can observe that the approximant $\phi_{33}^*(t)$ has already a rather good quality of approximation of the exact function. Relative percentage

errors for the Padé approximant $P_3^2(t)$ and for the self-similar exponential approximant $\phi_{55}^*(t)$ are shown in Fig. 13. In a narrow region, $P_3^2(t)$ outperforms $\phi_{55}^*(t)$ but fails short for larger times. However, due to the fact that the control parameters τ_2, τ_3, τ_4 and τ_5 remain all positive and of similar magnitude, the quality of $\phi_{55}^*(t)$ becomes eventually worse than that of the Padé approximation at very large times.

To investigate this behavior some more, let us construct the following function, $\phi(t) = \exp(-t\ (1+t)^{-1/2})$, which decays as $\exp(-\sqrt{t})$, as time goes to infinity. Its Taylor expansion, $\phi_5(t) \simeq \sum_{k=0}^{5} a_k\ t^k$ possesses the coefficients

$$a_0 = 1, \quad a_1 = -1, \quad a_2 = 1, \quad a_3 = -\frac{25}{24}, \quad a_4 = \frac{53}{48}, \quad a_5 = -\frac{2261}{1920}.$$

The control parameters,

$$\tau_2 = 0.5, \quad \tau_3 = 0.48, \quad \tau_4 = 0.393, \quad \tau_5 = 0.367,$$

are all positive, smaller than one but decrease rather slowly. Fig. 14 shows the dependence of the multipliers as a function of time. One can observe their poor convergence. As a consequence, the self-similar exponential approximants $\phi_{44}^*(t)$ and $\phi_{55}^*(t)$ bracket the exact function rather poorly, see Fig. 15, with an accuracy inferior to that of the Padé approximant $P_4^1(t)$, with the exception of very large times, see Fig. 16.

These two examples illustrate the property that, for coefficients a_i's rapidly growing in absolute values, the considered self-similar exponential approximants, with controls described by the accuracy-trough-order relationship, become unreliable. Such cases of coefficients growing as fast as a factorial of their order constitute an important class of behavior, since it appears in expansions that are typical to many nonlinear field theories. Consider for instance the particularly illustrative example of the Stieltjes function, $\phi(t) = \int_0^\infty \frac{\exp(-u)}{1+tu} du$, which exemplifies such a behavior. Its coefficients of the Euler series [28]

$$a_0 = 1, \quad a_1 = -1!, \quad a_2 = 2!, \quad a_3 = -\ 3!, \quad a_4 = 4!, \quad a_5 = -5!,$$

diverging as a factorial, lead to the control parameters

$$\tau_2 = 0.75, \quad \tau_3 = 0.713, \quad \tau_4 = 0.697, \quad \tau_5 = 0.685\ .$$

As we can anticipate from our previous observations, both the multipliers and approximants sequences are not convergent simultaneously, as seen in Figs. 17 and 18. In this case, the Padé approximant $P_3^2(t)$ easily outperforms $\phi_{55}^*(t)$, see Fig. 19.

We stress that this failure of the Euler-type self-similar exponential approximants, as compared to the Padé approximants, does not imply the failure of the algebraic self-similar renormalization as a whole. Rather, it demonstrates the limitations of the particular way of defining controls and also of the infinite-power condition ($s \to \infty$) used in the derivation of these approximants. In applications, the usage of the exponential approximants is often analogous to mean-field-type approximations. Because of this, we may call, for brevity, the limit $s \to \infty$ as the mean-field condition. It is important to realize that this mean-field theory sends clear warnings about its own anticipated failure, reflected in the divergent behavior of the approximants and of their multipliers. In a subsequent paper, we show that lifting of the infinite-power restriction improves dramatically the accuracy of the self-similar renormalization.

IV. EXPONENTIAL APPROXIMANTS DERIVED FROM A DIFFERENTIAL EQUATION

We end our exploration of illustrative examples by the analysis of an expansion derived from the time evolution equation of the state variable usually called θ in the friction literature of a block subjected to constant shear over normal stress, given by the Ruina-Dieterich solid friction law (see [29] page 283 section 13.6.2 and [30,31]). Posing $x \equiv \theta/\theta_0$ where θ_0 is a parameter of the constitutive friction law, the following equation

$$\frac{dx}{dt} = \theta_0^{-1} - \alpha\, x^{1-m}, \qquad x(0) = x_0 > 0\ , \tag{9}$$

describes the evolution of the state variable of the friction law. In the following, we shall consider the case when the condition $\theta_0^{-1} - \alpha x_0^{1-m} < 0$ holds which ensures that the solid friction state variable tends to decrease from an initial large value. This law (9) results from

a velocity-dependent solid friction coefficient, the block velocity V being related to the state variable x by the relation $V \propto 1/x^m$. α is a parameter of the constitutive velocity-dependent solid friction law. The exponent m is also a parameter dependent upon the physical nature of the solid contacts. Equation (9) with initial condition $\theta_0^{-1} - \alpha x_0^{1-m} < 0$ thus describes the acceleration of a block in contact with a solid substrate pulled with a constant force which has been suddenly applied at $t = 0$. It has been applied to describe one of the possible regimes of a mountainous slope which can become transiently unstable [31].

In dimensionless variables, $X = x/\overline{x}, \quad T = t/\overline{t}$, where

$$\overline{x} = (\alpha\theta_0)^{\frac{1}{m-1}} , \qquad \overline{t} = |1-m|^{-1} \, \alpha^{\frac{1}{m-1}} \theta_0^{\frac{m}{m-1}} , \tag{10}$$

Eq. (9) reads,

$$\frac{dX}{dT} \; (|1-m|) = 1 - \; X^{1-m}, \qquad X(0) = X_0 = \frac{x_0}{\overline{x}}, \qquad 1 - X_0^{1-m} < 0 \; . \tag{11}$$

For $m < 1$, it is a nonlinear relaxation equation, with $\overline{x}$ being an equilibrium value reached asymptotically after an exponential decay characterized by the typical time $\overline{t}$. For $m < 1$, in a long-time limit, we obtain an asymptotic solution in the form,

$$x(t) \simeq \overline{x} + A_1 \exp\left(-t/\overline{t}\right) + ..., \qquad t \to \infty \; , \tag{12}$$

where the value of A_1 remains unknown. A naive approach consists then in writing down a naive approximate solution to Eq. (9), $x_N(t)$, based on such an asymptotic single relaxation time expression,

$$x_N(t) = \overline{x} + (x_0 - \overline{x}) \exp\left(-t/\overline{t}\right) \; . \tag{13}$$

In this ansatz, the amplitude A_1 is now determined.

The exact expansion $x_k(t)$ up to order t^k for short times and arbitrary m can be obtained from Eq. (9). Here, we limit ourselves to expansion up to the fifth order,

$$x_5(t) \simeq \sum_{n=0}^{5} a_n t^n, \; t \to 0, \tag{14}$$

where in dimensional units,

$$a_0 = x_0, \quad a_1 = \theta_0^{-1} - \alpha\ x_0^{1-m}, \quad a_2 = \frac{1}{2}\alpha\ (m-1)\ a_1 x_0^{-m},$$

$$a_3 = \frac{1}{6}\alpha(m-1)\left[-m\ a_1^2\ x_0^{-m-1} + 2a_2\ x_0^{-m}\right],$$

$$a_4 = \frac{1}{24}\alpha(m-1)\left[(1+m)\ \ m\ a_1^3\ x_0^{-m-2} - 6m\ a_2\ a_1 x_0^{-m-1} + 6a_3\ x_0^{-m}\right],$$

$$a_5 = \frac{1}{5!}\alpha(m-1)\left[-m(1+m)(2+m)a_1^4 x_0^{-m-3} + 12m(1+m)x_0^{-m-2}a_1^2 a_2 - \right.$$

$$\left. -24m x_0^{-m-1} a_3 a_1 - 12m x_0^{-m-1} a_2^2 + 24 x_0^{-m} a_4\right].$$

Using this expansion, we apply our technique to construct a self-similar exponential approximant using this fifth-order expansion (14). For $m = 0.85$, $X_0 = 50$, Fig. 20 illustrates how well the "exact" numerical solution is approximated by superexponential approximants in dimensionless units. The values of the control parameters,

$$\tau_2 = -2.02, \quad \tau_3 = 1.504, \quad \tau_4 = 0.848, \quad \tau_5 = 0.649,$$

have different signs, with τ_2 and τ_3 being rather large, which leads to a limited quality of the approximations at different orders. We stress that these values for the model parameters correspond to a highly nonlinear and strongly out-of-equilibrium case, where the naive exponential expression $x_N(t)$, corresponding to a close-to-equilibrium linearized model is way-off the mark both in qualitative and quantitative sense, see Fig. 20. In order to guarantee that the solution saturates at the correct constant value at infinite time, we add and subtract $\overline{x}$ from the initial series, which produces a single modification in that only a_0 is replaced by $a_0 - \overline{x}$ in the generic expressions for the approximants. We thus plot

$$x(t) = \overline{x} + x_{ii}^*(t),\ \ i = 2, 3, ...5\ , \tag{15}$$

divided by $\overline{x}$ as a function of the dimensionless time T. Note that such shifts are completely compatible with the framework of algebraic self-similar renormalization, see e.g. Ref. [20]. For the fifth-order approximant studied here, the relative error is largest around $T = 12.57$ and amounts to 1%.

In order to compare the accuracy of the self-similar approximants with the Padé approximants [28], we consider the Padé approximant,

$$P_3^3(t) = \frac{a_0 + A_1 t + A_2 t^2 + B_3 \overline{x} t^3}{1 + B_1 t + B_2 t^2 + B_3 t^3} \; , \tag{16}$$

which goes to $\overline{x}$ at infinity, with all unknown coefficients determined from the short time expansion (14). Fig. 21 shows that $P_3^3(t)$ completely fails at intermediate times and even goes through singularity before returning to asymptotic value $\overline{x}$ at large times.

In summary, in this case, the self-similar exponential approximant has been able to capture a highly non-trivial departure from a pure exponential relaxation which is dominating the relaxation process over a large time span, conditioned on the fact that the relaxation becomes asymptotically an exponential at long times. This shows again the power of this resummation method to capture significant deviations from exponentials in functions that belong to the exponential class in an asymptotic sense.

V. CONCLUDING REMARKS

In conclusion, we have demonstrated how the technique of self-similar exponential approximants makes it possible to reconstruct exponential-type functions, when only a few terms of their expansions are known.

This technique can also be applied to functions with asymptotic behavior different from an exponential. In this case, by carefully examining the convergence of the multipliers and of the approximants, it is possible to construct an accurate approximation for the sought function, while staying within the limits of applicability of the mean-field regime.

Further increase of accuracy will come from lifting the mean-field condition used in deriving the self-similar exponential approximants. The result of this approach will be presented elsewhere.

The Padé approximants remain a valuable technique, but it has no much value in theories of relaxation and should be replaced by other techniques, possibly by the superexponentials presented here and their non mean-field extensions that we shall report in a future work.

REFERENCES

[1] A. Johansen and D. Sornette, Phys. Rev. Lett. **82**, 5152 (1999).

[2] D. Sornette and L. Knopoff, Bull. Seism. Soc. Am. **87**, 789 (1997).

[3] A.S. Parkins and D.F. Walls, Phys. Rep. **303**, 1 (1998).

[4] F. Dalfovo, S Giorgini, L.P. Pitaevskii, and S. Stringari, Rev. Mod. Phys. **71**, 463 (1999).

[5] P.W. Courteille, V.S. Bagnato, and V.I. Yukalov, Laser Phys. **11**, 659 (2001).

[6] T.L. Ho, Phys. Rev. Lett. **81**, 742 (1998).

[7] C.K. Law, H. Pu, and N.P. Bigelow, Phys. Rev. Lett. **81**, 5257 (1998).

[8] A. Abragam, *Principles of Nuclear Magnetism* (Clarendon, Oxford, 1961).

[9] A. Abragam and M. Goldman, *Nuclear Magnetism: Order and Disorder* (Clarendon, Oxford, 1982).

[10] F. Hartmann-Bourton, P. Politi, and J. Villain, Int. J. Mod. Phys. B **10**, 2577 (1996).

[11] B. Barbara, L. Thomas, F. Lionti, I. Chiorescu, and S. Sulpice, J. Magn. Magn. Mat. **200**, 167 (1999).

[12] A. Caneschi et. al., J. Magn. Magn. Mat. **200**, 182 (1999).

[13] Z.-K. Shen, D.D. Jackson, Y. Feng, M. Cline, M. Kim, P. Fang and Y. Bock, Bull. Seism. Soc. Am. **84**, 780 (1994).

[14] D. Massonnet, K. Feigl, M. Rossi and F. Adragna, Nature **369**, 227 (1994).

[15] V.I. Yukalov and S. Gluzman, Phys. Rev. E **58**, 1359 (1998).

[16] C.M. Bender and J.P. Vinson, J. Math. Phys. **37**, 4103 (1996).

[17] S. Gluzman and V.I Yukalov, Phys. Rev. E **55**, 3983 (1997).

[18] V.I Yukalov and S. Gluzman, Phys. Rev. E **55**, 6552 (1997).

[19] V.I Yukalov and S. Gluzman, Phys. Rev. Lett. **79**, 333 (1997).

[20] S. Gluzman and V.I Yukalov, Phys. Rev. E **58**, 4197 (1998).

[21] V. I. Yukalov and S. Gluzman, Int. J. Mod. Phys. B **13**, 1463 (1999).

[22] V.I. Yukalov, Physica A **167**, 833 (1990).

[23] V.I. Yukalov, J. Math. Phys. **32**, 1235 (1991).

[24] V.I. Yukalov, J. Math. Phys. **33**, 3994 (1992).

[25] V.I. Yukalov and E.P. Yukalova, Ann. Phys. (N.Y.) **277**, 219 (1999).

[26] L. Euler, Acta Acad. Petropolitanae **1**, 38 (1777).

[27] R.A. Knoebel, Am. Math. Monthly **88**, 235 (1981).

[28] G.A. Baker and P. Graves-Morris, *Padé Approximants* (Cambridge University, Cambridge, 1996).

[29] D. Sornette, Critical Phenomena in Natural Sciences (Chaos, Fractals, Self-organization and Disorder: Concepts and Tools) (Springer Series in Synergetics, Heidelberg, 2000).

[30] J.H. Dieterich, Tectonophysics **211**, 115 (1992).

[31] A. Helmstetter, J.V. Andersen, S. Gluzman, J.-R. Grasso, and D. Sornette, Block friction model, finite-time singularities and prediction of catastrophic landslides (in preparation).

Figure Captions

Figure 1. The conventional Padé approximants, $P_3^2(t)$ (dash-dot) and $P_4^1(t)$ (dash) compared with $exp(-t)$ (solid). Approximant $\phi_{51}^*(t)$ (dot) is shown as well.

Figure 2. The relative percentage errors for the $P_3^2(t)$ (solid) and $P_4^1(t)$ (dash) Padé approximants, are shown. One should not be mislead by the seemingly superior performance of $P_4^1(t)$, which is qualitatively wrong in predicting negative values already for moderate times.

Figure 3. Illustration of the impact of "noise" η (or θ) in the coefficients of the power law expansion, onto the accuracy of the exponential approximant ϕ_{22}^*, characterized by the absolute error, $\phi_{22}^*(t,\eta,0) - \phi_{22}^*(t) \simeq b_1(t)\ \eta + b_2(t)\ \eta^2 + ...$ and $\phi_{22}^*(t,0,\theta) - \phi_{22}^*(t) \simeq c_1(t)\ \theta + c_2(t)\ \theta^2 +$. The absolute errors in the lowest order,$|b_1(t)|$ (solid) and $c_1(t)$ (dash), are shown as functions of time ($\eta = \theta = 1$).

Figure 4. Demonstration of the influence of the noise introduced into the higher order terms in the expansion onto the absolute error dependence on time. The absolute errors in the lowest order,$|b_1(t)|\ \eta$ (solid), the next order contribution to the error, $b_2(t)\ \eta^2$ (dashed), and their sum (dotted line) are shown for $\eta = 0.1$. Same notations as in Fig. 3.

Figure 5. It is impossible to distinguish the approximant $\phi_{55}^*(t)$ (dash-dot) from the exact function, $\phi(t) = \sin(t)^2 \exp(-t^2)$, intended to be shown with dots. Approximants $\phi_{41}^*(t)$ (solid line), $\phi_{51}^*(t)$ (dash line) and Taylor expansions $\phi_{55}(t)$ (short dot) and $\phi_{44}(t)$ (dash-dot-dot) are presented for comparison as well.

Figure 6. The logarithms of the relative percentage errors for the Padé approximant $P_3^2(x)$ (dash) and for the super-exponential approximant $\phi_{55}^*(t)$ (solid), in the case of $\phi(t) = \sin(t)^2 \exp(-t^2)$.

Figure 7. Multipliers $M_{22}^*(t)$ (dash-dot), $M_{33}^*(t)$ (dot), $M_{44}^*(t)$ (dash), $M_{55}^*(t)$ (solid

line) in the case of $\phi(t) = \ln(1+t)\exp(-t^2)$.

Figure 8. The self-similar exponential approximants $\phi^*_{44}(t)$ (dashed line) and $\phi^*_{55}(t)$ (solid line), bracket the exact function $\phi(t) = \ln(1+t)\exp(-t^2)$, shown with dash-dot-dot. The approximants $\phi^*_{22}(t)$ (dash-dot line) and $\phi^*_{33}(t)$ (dotted line) are presented as well.

Figure 9. The Padé approximants $\mathrm{P}^2_3(t)$ (dash), $\mathrm{P}^1_4(t)$ (solid), $\mathrm{P}^4_1(t)$ (dash-dot), $\mathrm{P}^3_2(t)$ (dot) and $\phi^*_{55}(t)$ (short dot) are compared to each other and with the exact $\phi(t) = \ln(1+t)\exp(-t^2)$ (dash-dot-dot).

Figure 10. Logarithm of the relative percentage errors for the self-similar exponential approximant $\phi^*_{55}(t)$ (solid line) and for the Padé approximant $\mathrm{P}^4_1(t)$ (dash), in the case of $\phi(t) = \ln(1+t)\exp(-t^2)$.

Figure 11. The dependence of the multipliers $M^*_{22}(t)$ (dash-dot), $M^*_{33}(t)$ (dot), $M^*_{44}(t)$ (dash), $M^*_{55}(t)$ (solid)as a function of time, in the case of $\phi(t) = \frac{1}{1+t}\exp(-t)$

Figure 12. The approximants $\phi^*_{33}(t)$ (dot), $\phi^*_{44}(t)$ (dash), $\phi^*_{55}(t)$ (solid) are compared to the exact function $\phi(t) = \frac{1}{1+t}\exp(-t)$ (dash-dot).

Figure 13. The relative percentage errors for the Padé approximant $\mathrm{P}^2_3(x)$ (dash) and for the self-similar exponential approximant $\phi^*_{55}(t)$ (solid) are shown in the case of $\phi(t) = \frac{1}{1+t}\exp(-t)$.

Figure 14. Dependence of the multipliers $M^*_{22}(t)$ (dash-dot), $M^*_{33}(t)$ (dot), $M^*_{44}(t)$ (dash), $M^*_{55}(t)$ (solid line) as a function of time in the case of $\phi(t) = \exp(-t\ (1+t)^{-1/2})$.

Figure 15. The self-similar exponential approximants $\phi^*_{44}(t)$ (dashed line) and $\phi^*_{55}(t)$ (solid line), bracket the exact function $\phi(t) = \exp(-t\ (1+t)^{-1/2})$ shown with dash-dot-dot, rather poorly. Approximants $\phi^*_{22}(t)$ (dash-dot line) and $\phi^*_{33}(t)$ (dotted line) are presented as well.

Figure 16. Error of the approximant $\phi^*_{55}(t)$ (solid line) in the case of $\phi(t) = \exp(-t\ (1+t)^{-1/2})$, compared with that of the Padé approximant $P^1_4(t)$, shown with dashed line.

Figure 17. Multipliers $M^*_{22}(t)$ (dash-dot), $M^*_{33}(t)$ (dot), $M^*_{44}(t)$ (dash), $M^*_{55}(t)$ (solid line) in the case of the Stieltjes function.

Figure 18. Approximants $\phi^*_{55}(t)$ (solid line) and $\phi^*_{44}(t)$ (dashed line) to the Stieltjes function, are compared with the exact expression (dash-dot line) and with the Padé approximant $P^2_3(t)$, shown with dotted line.

Figure 19. In the case of Stieltjes function, it is shown here that the Padé approximant $P^2_3(t)$ shown with dashed line, easily outperforms $\phi^*_{55}(t)$ shown with solid line

20. Illustration of how well the "exact" numerical solution to Eq. (11), can be approximated by the superexponential approximants in dimensionless units X and T , for $X(0) = 50,\ m = 0.85$. The "Exact" numerical solution to the Eq. (11) is shown as the solid line; the second -order approximation (15) is shown as the dash-dot-dot line; the third order approximation is shown as the dash-dot line; the fourth order approximation is shown with dotted line, while the best, fifth-order approximation, is shown with the dashed line and can barely be distinguished from the exact solution. The naive exponential expression $x_N(t)$ (13) is shown with the short dash line.

Figure 21. Demonstration that the two-point Padé approximant $P^3_3(t)$ (16) shown with dashed line, completely fails at intermediate times. The approximate solution (15), based on the fifth-order superexponential approximant and shown with solid line, works well.

Fig. 1

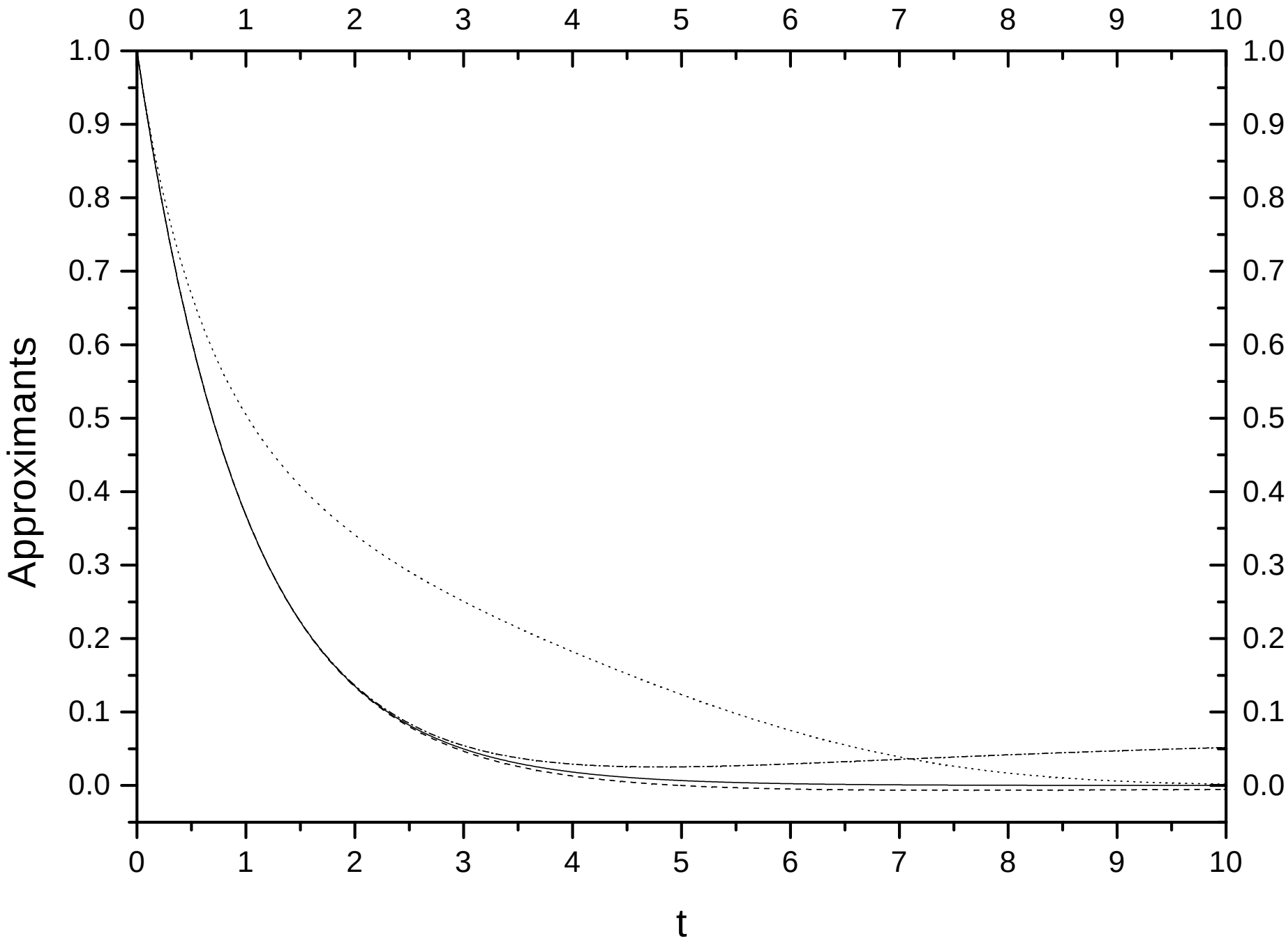

Fig. 2

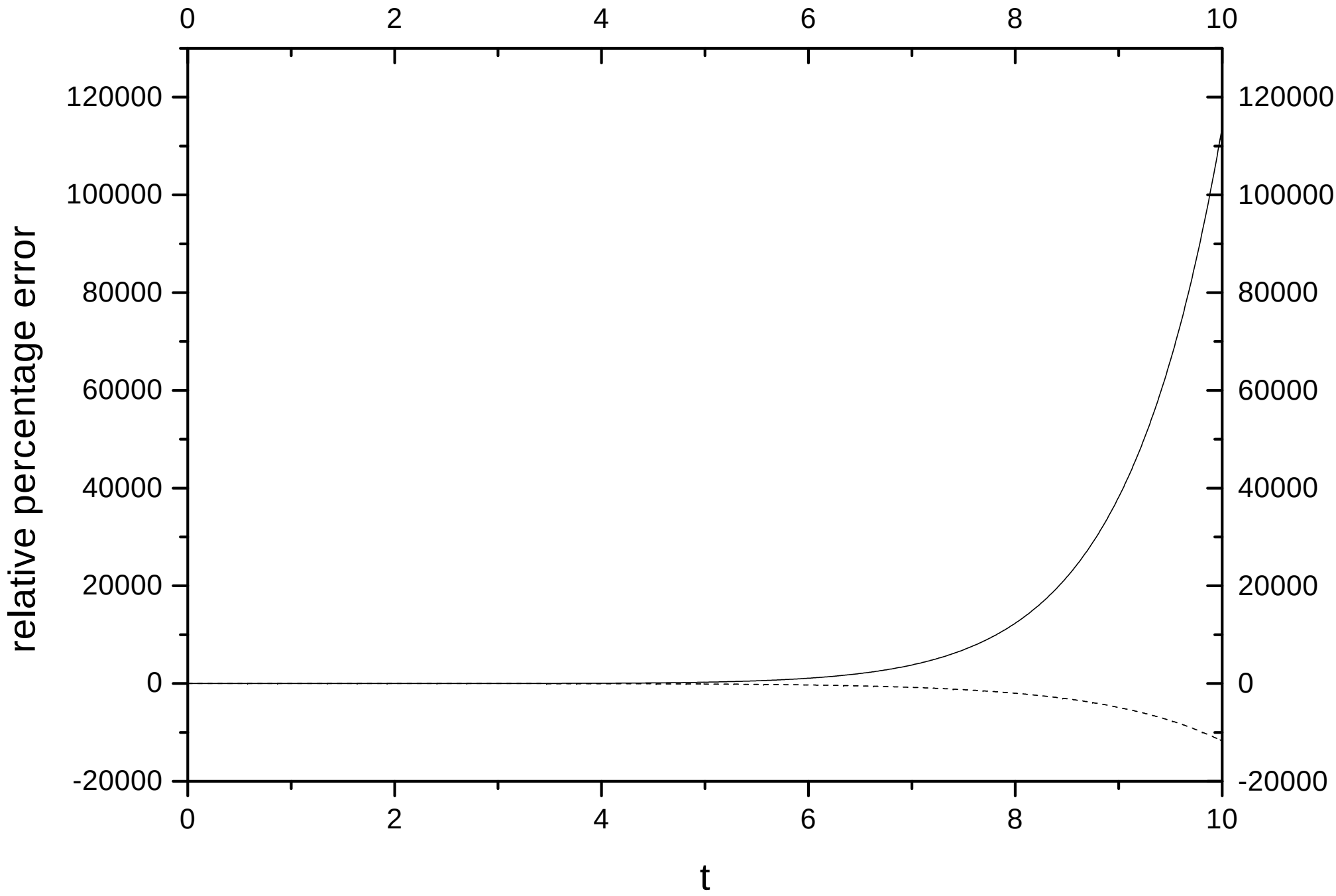
0
2
4
6
8
10
120000
100000
80000
60000
40000
20000
0
-20000
relative percentage error
t

Fig. 3

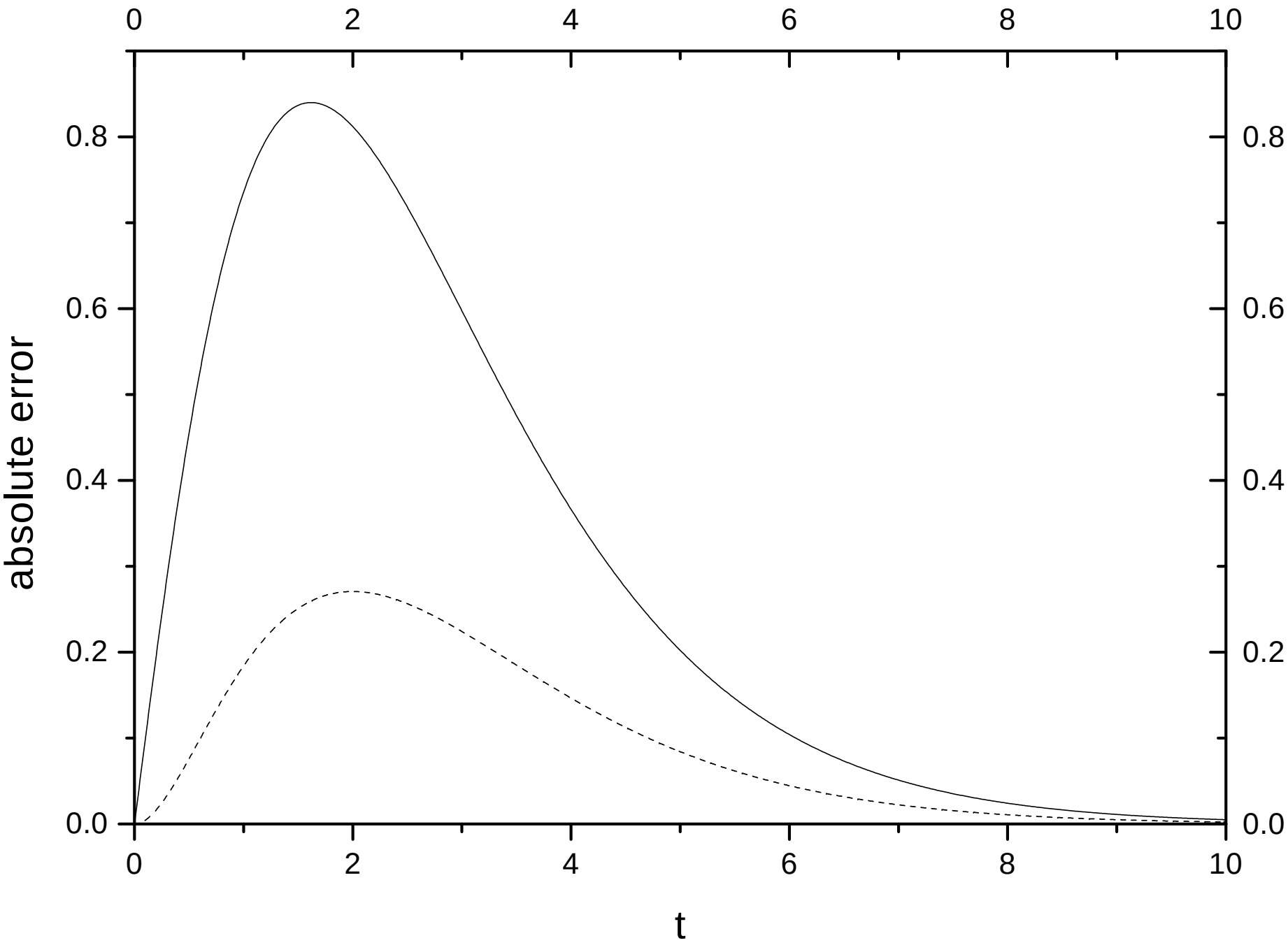

Fig. 4

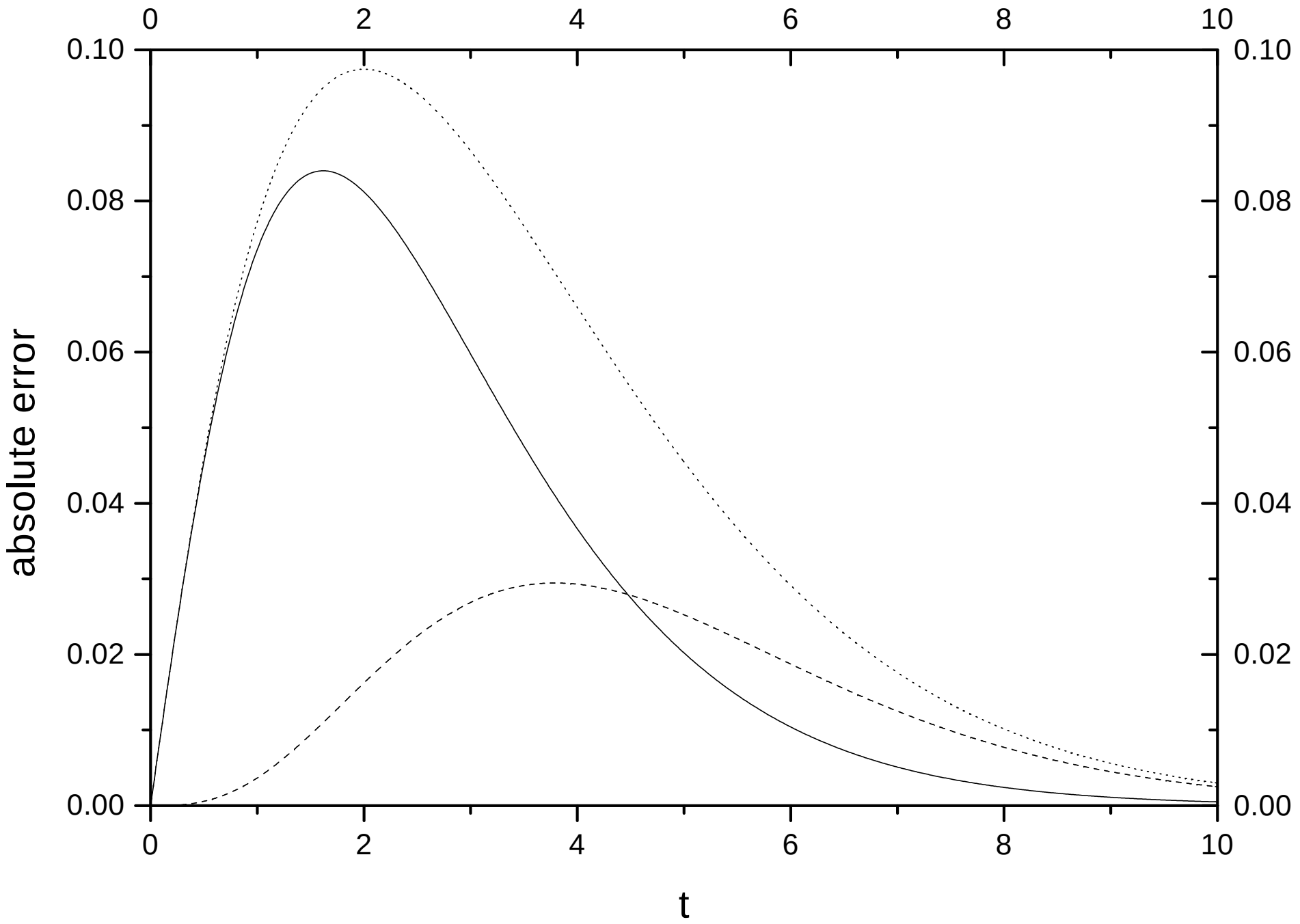

Fig. 5

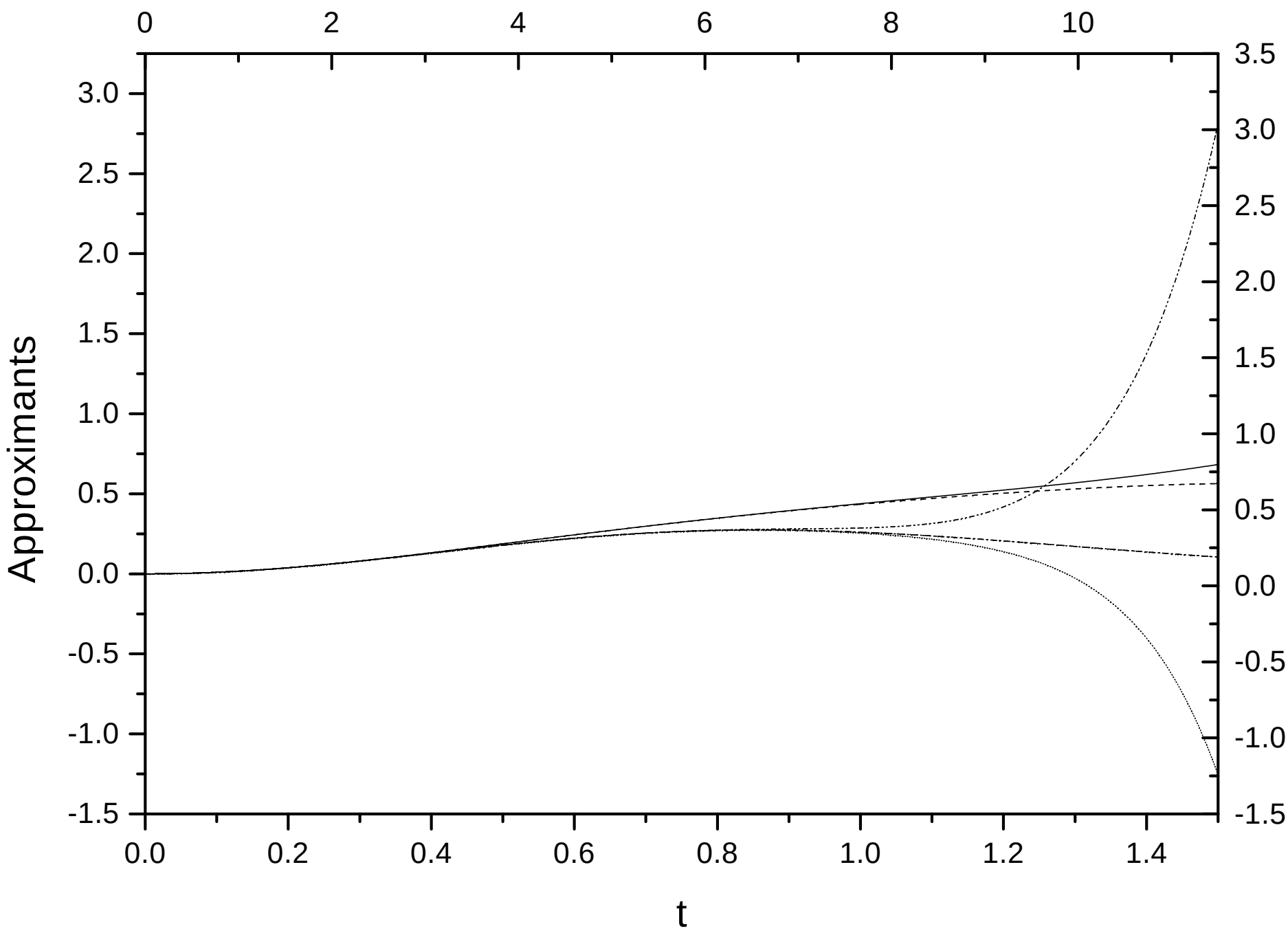
0
2
4
6
8
10
3.5
3.0
2.5
2.0
1.5
1.0
0.5
0.0
-0.5
-1.0
-1.5
Approximants
0.0
0.2
0.4
0.6
0.8
1.0
1.2
1.4
t

Fig. 6

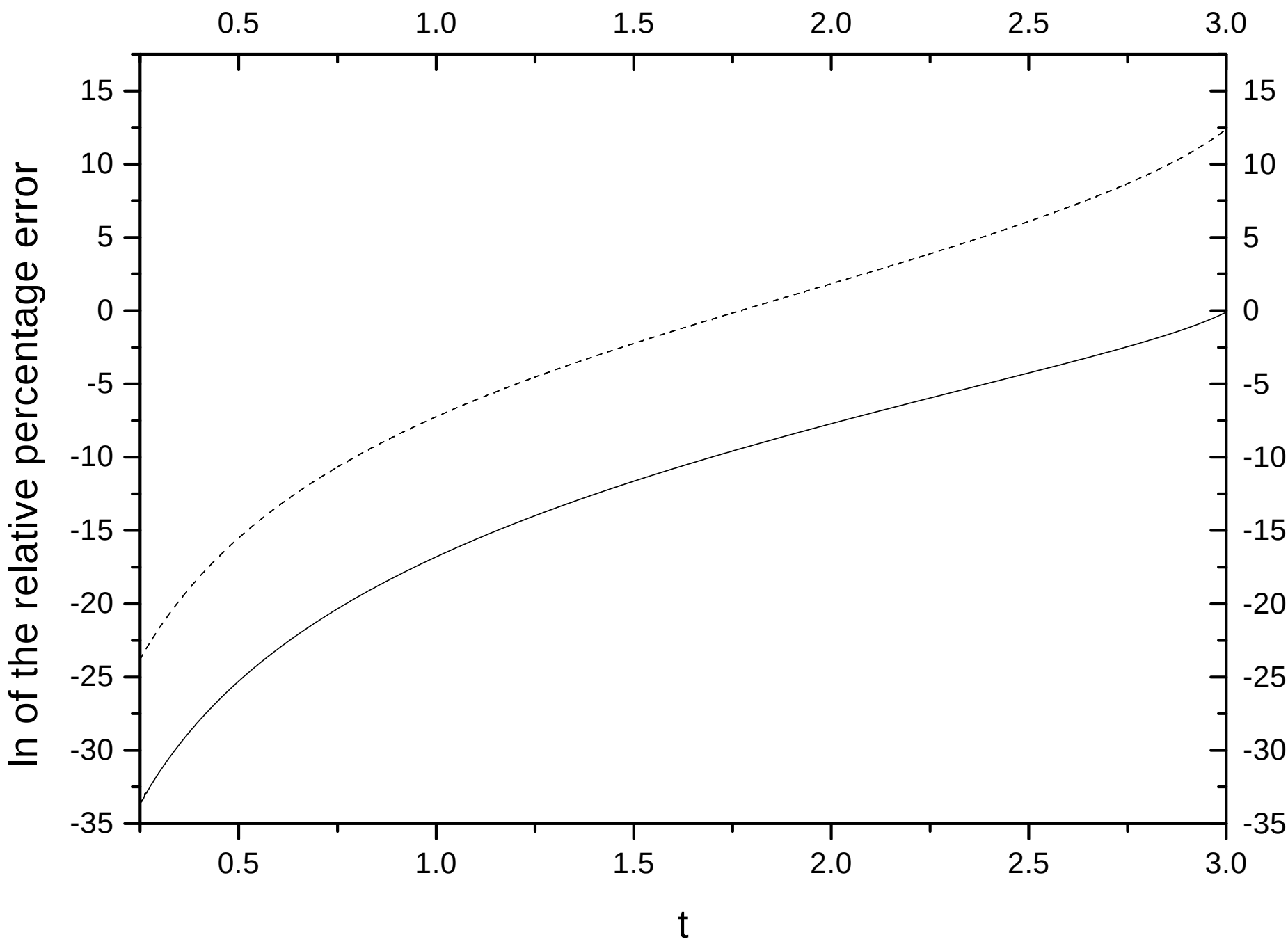
0.5
1.0
1.5
2.0
2.5
3.0
15
10
5
0
-5
-10
-15
-20
-25
-30
-35
ln of the relative percentage error
t

Fig. 7

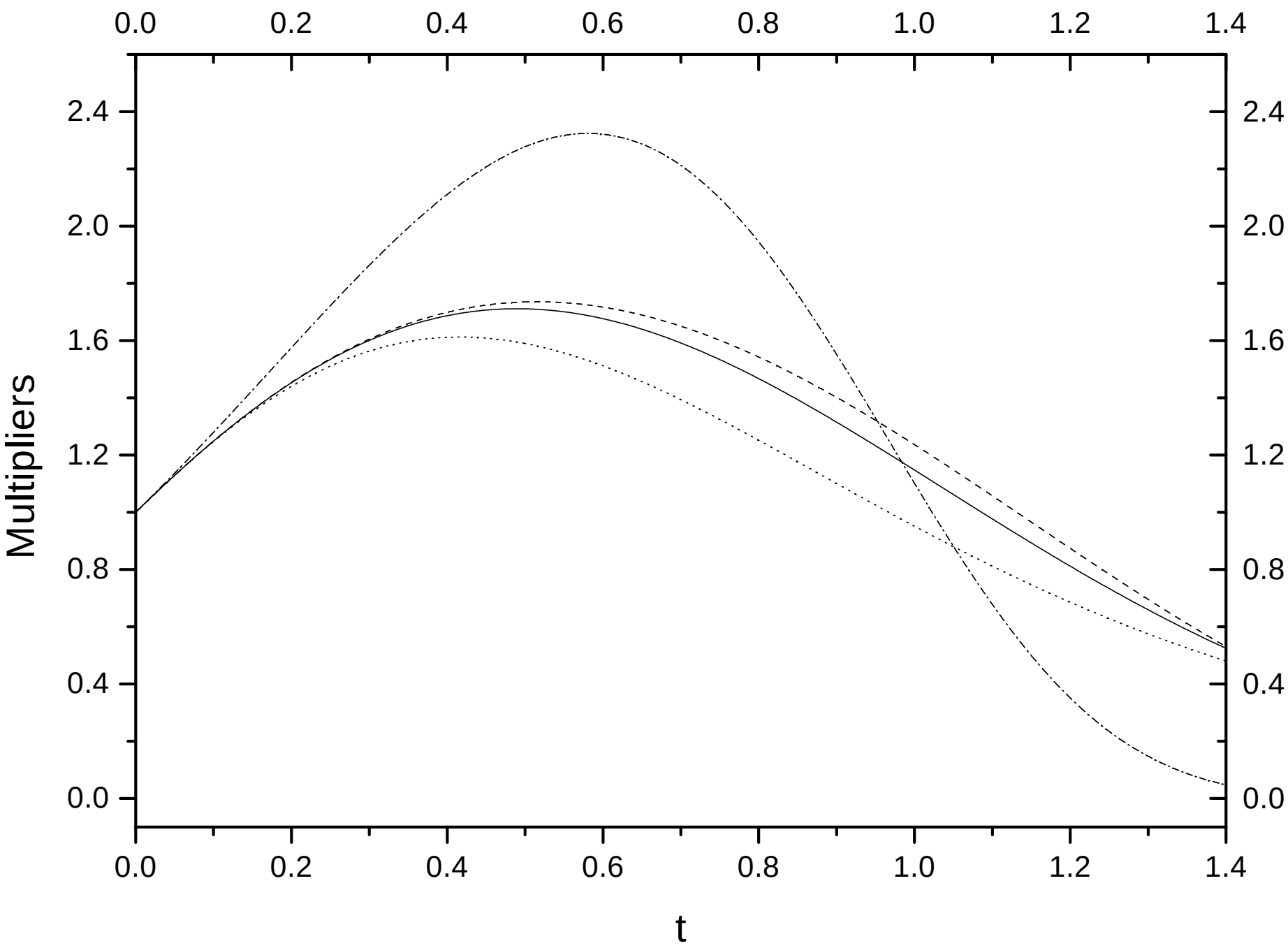

Fig. 8

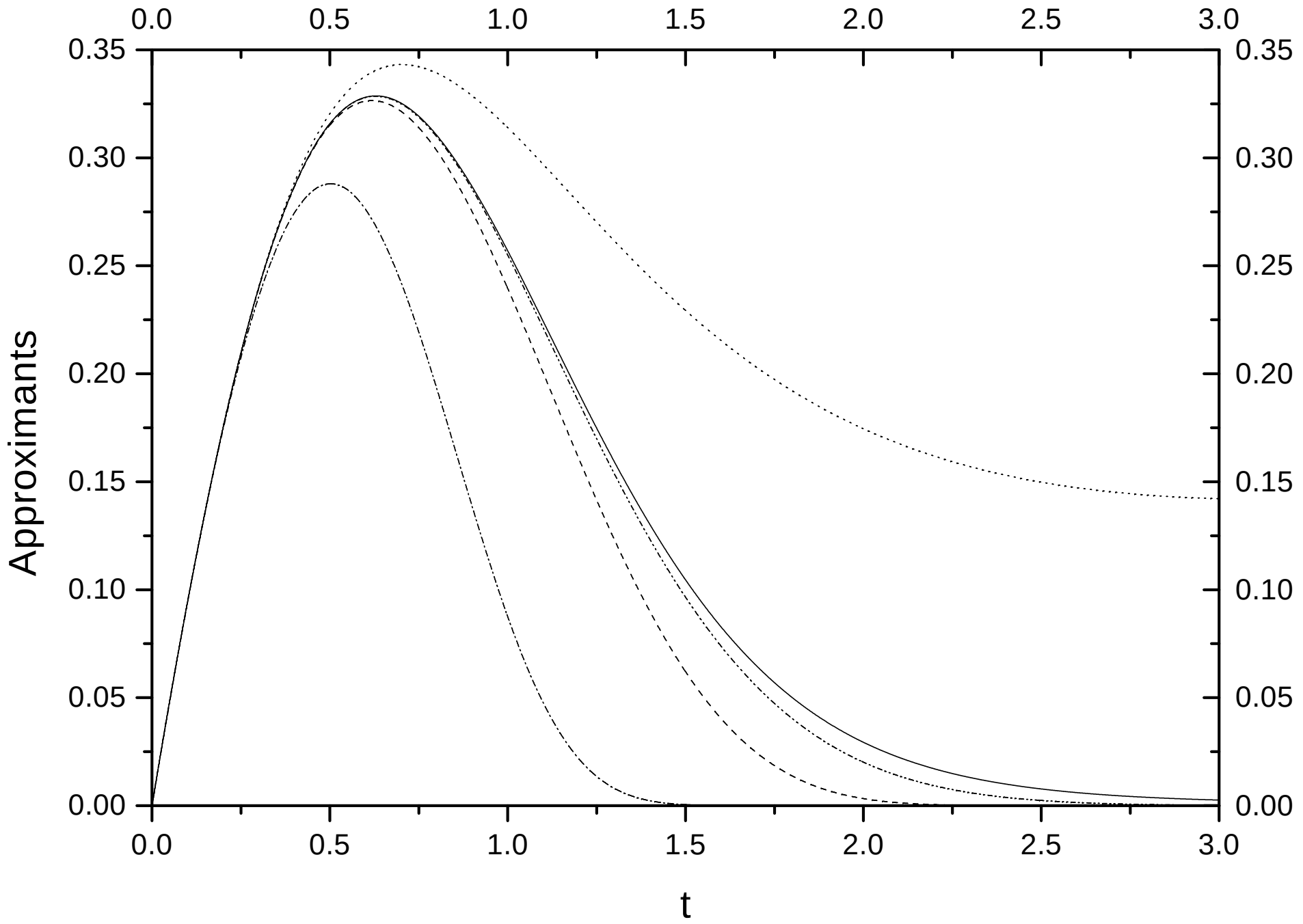
0.0
0.5
1.0
1.5
2.0
2.5
3.0
0.35
0.30
0.25
0.20
0.15
0.10
0.05
0.00
Approximants
t

Fig. 9

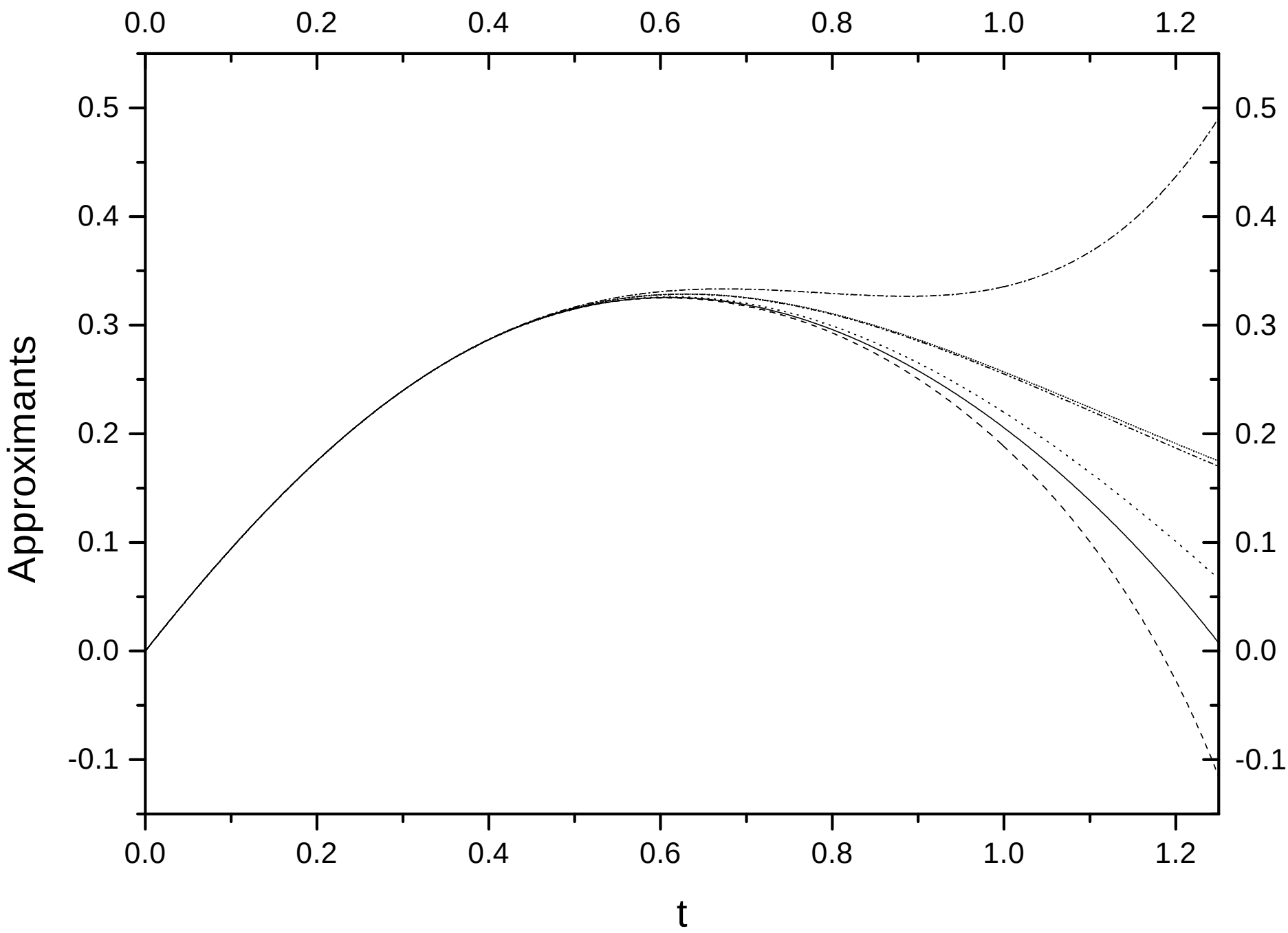

Fig. 10

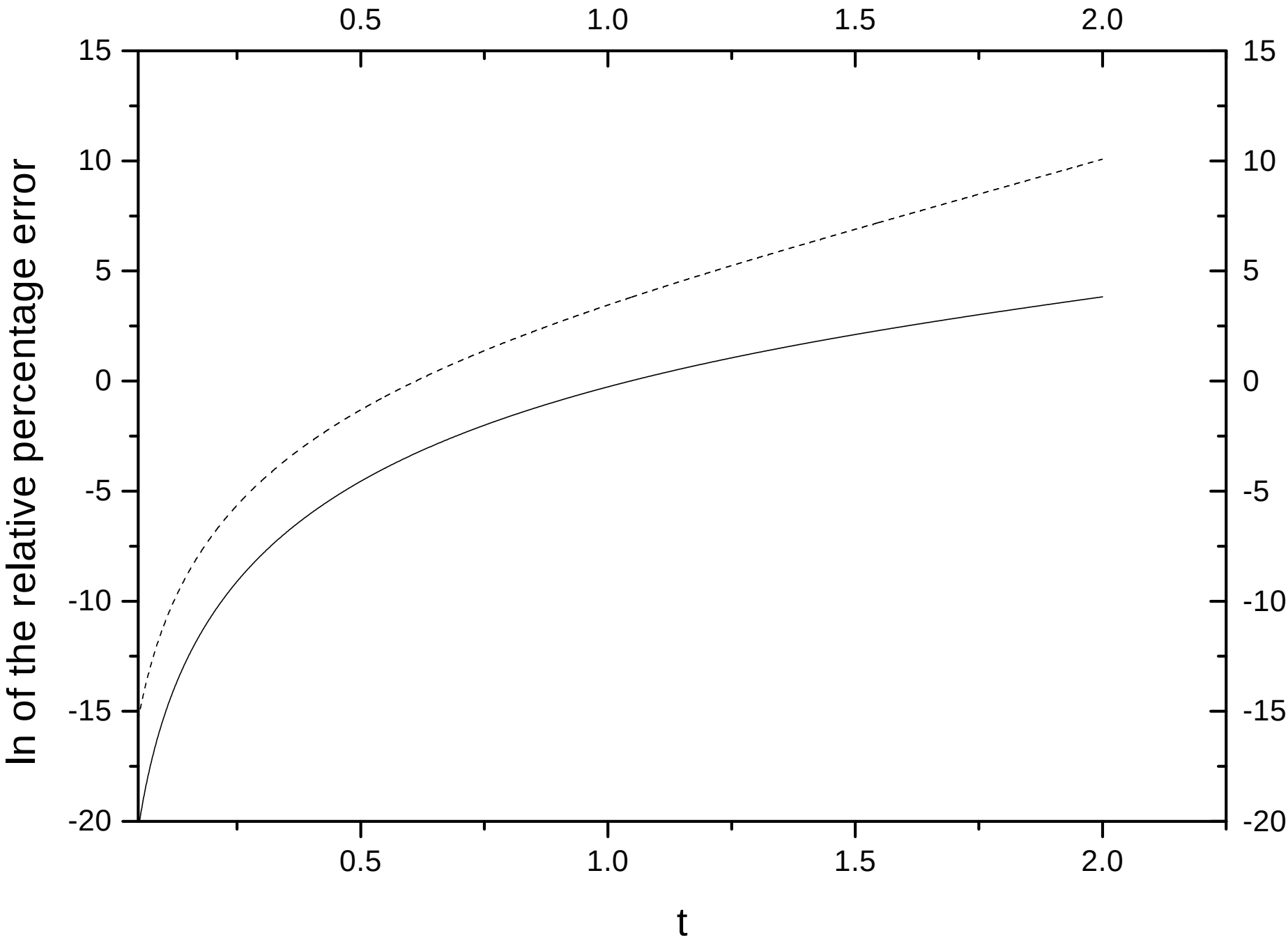
0.5
1.0
1.5
2.0
15
10
5
0
-5
-10
-15
-20
ln of the relative percentage error
t

Fig. 11

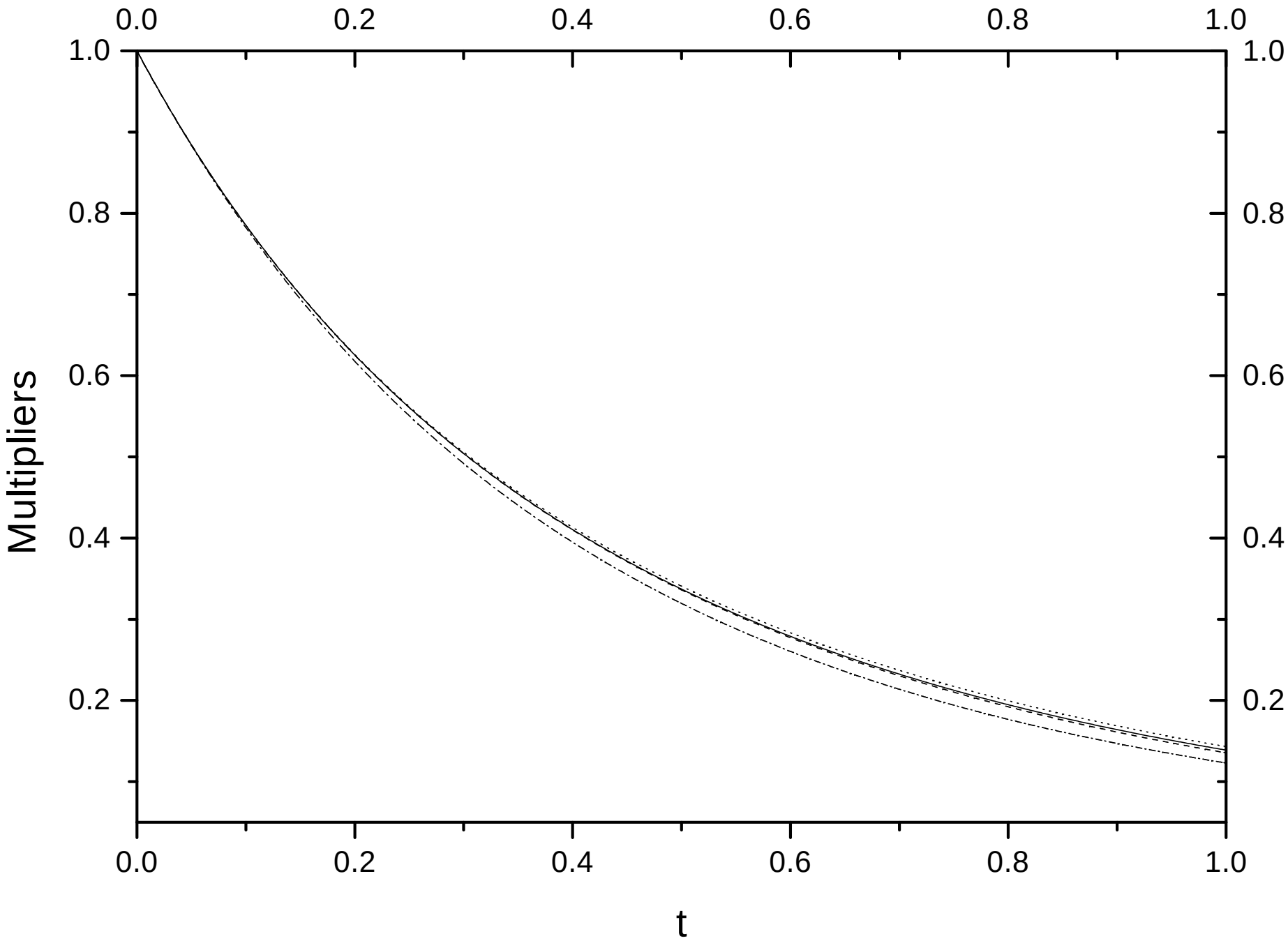

Fig. 12

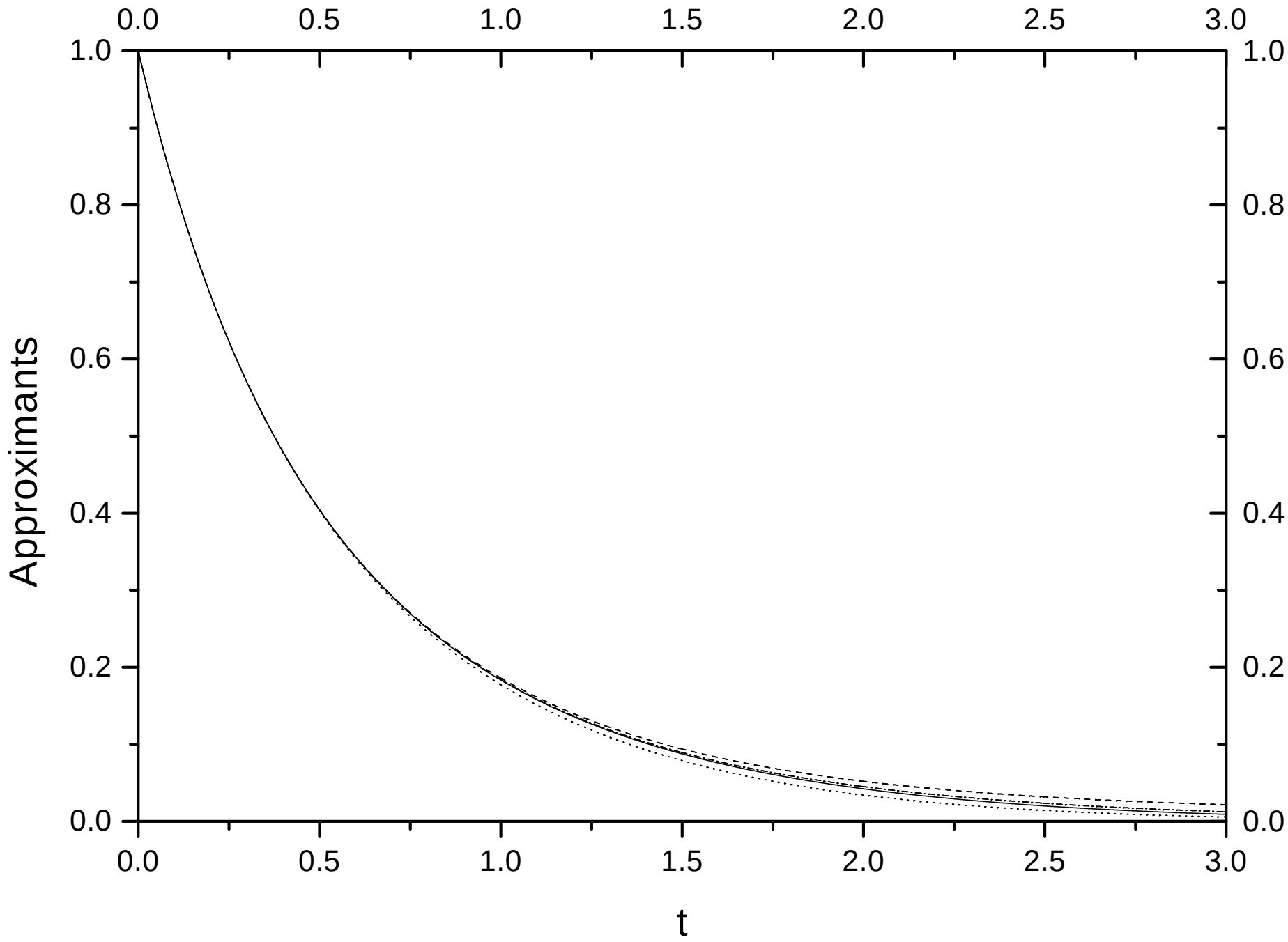

Fig. 13

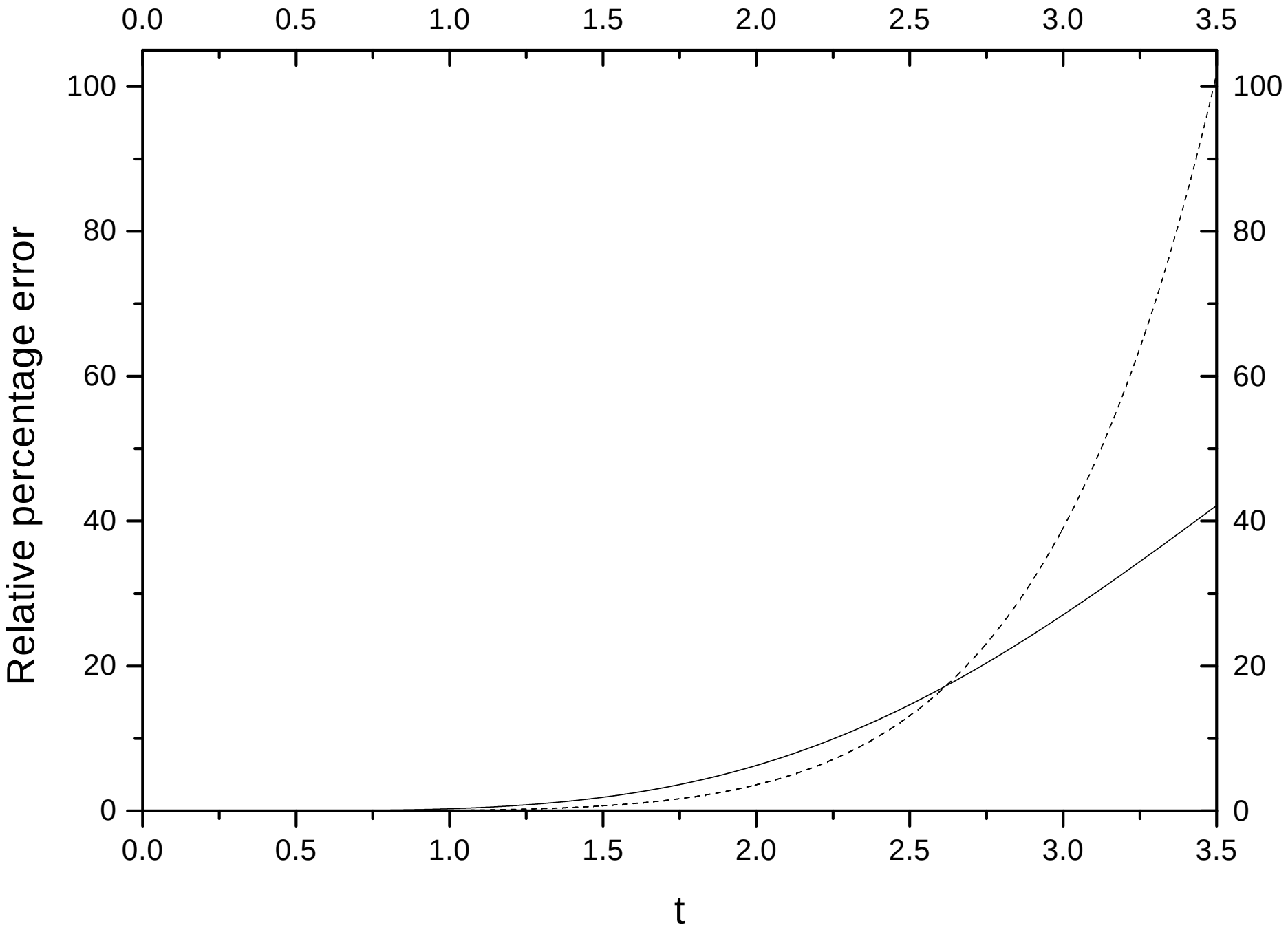
0.0
0.5
1.0
1.5
2.0
2.5
3.0
3.5
100
80
60
40
20
0
Relative percentage error
t

Fig. 14

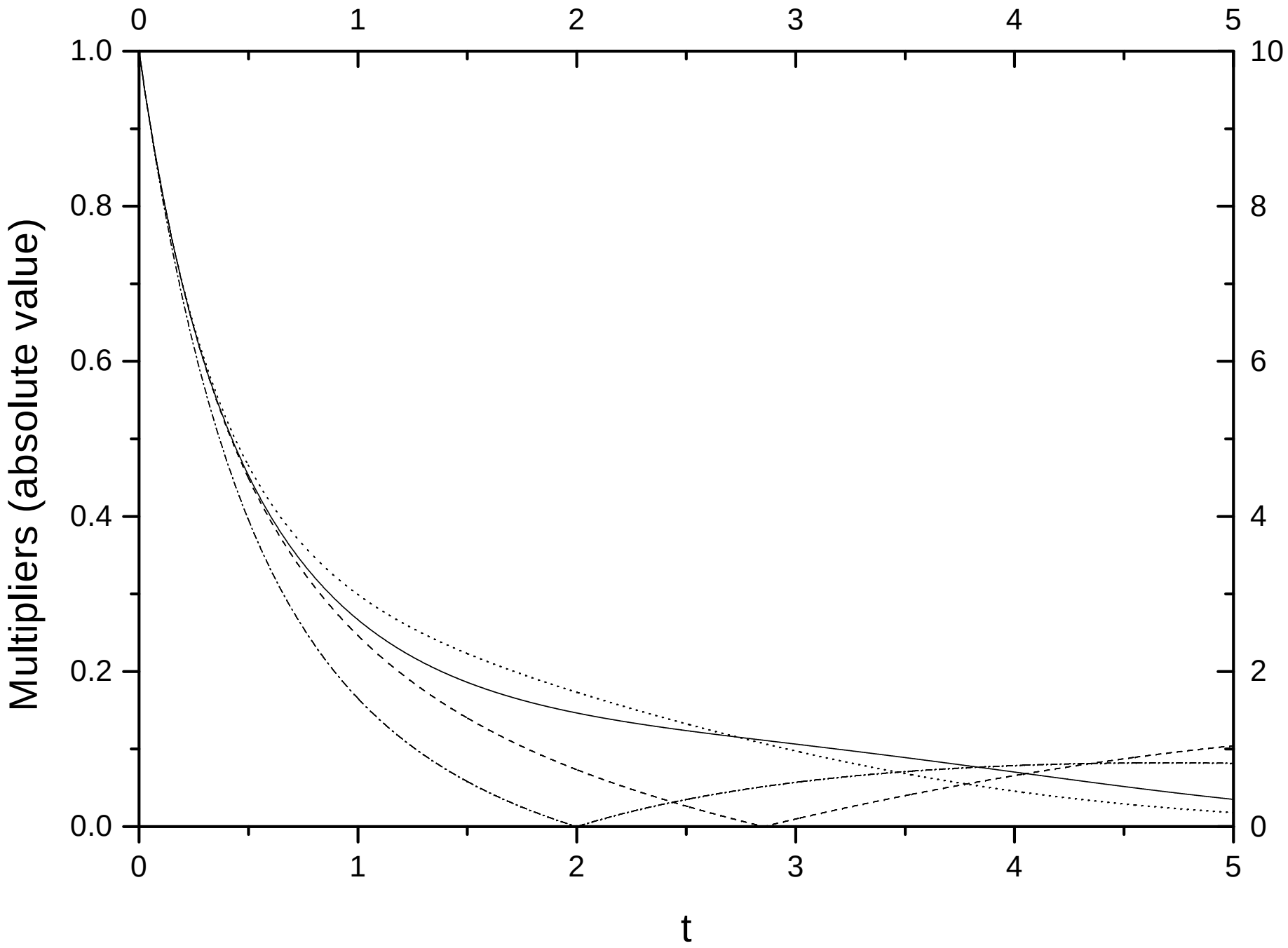
0
1
2
3
4
5
1.0
0.8
0.6
0.4
0.2
0.0
10
8
6
4
2
0
Multipliers (absolute value)
t

Fig. 15

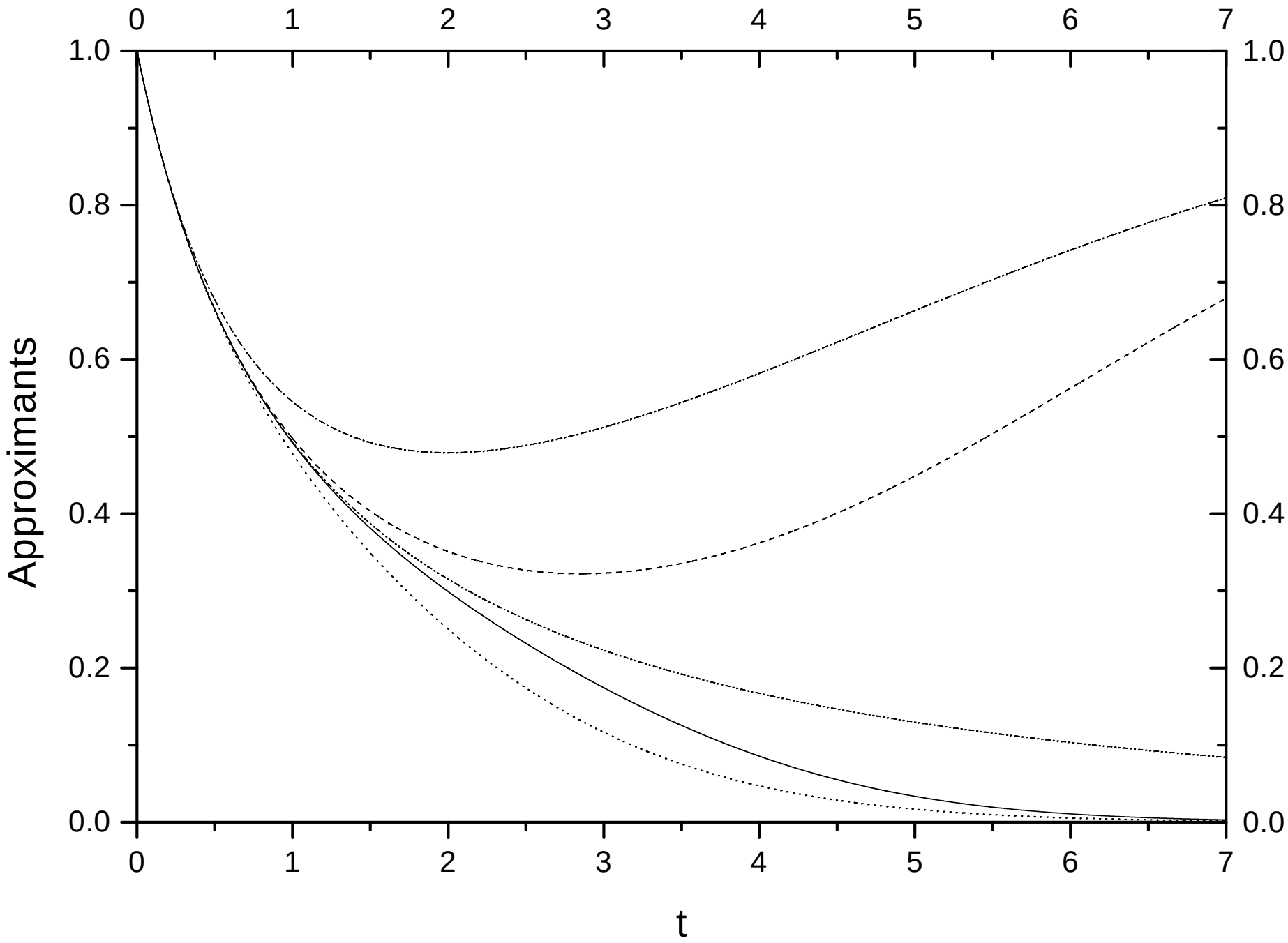

Fig. 16

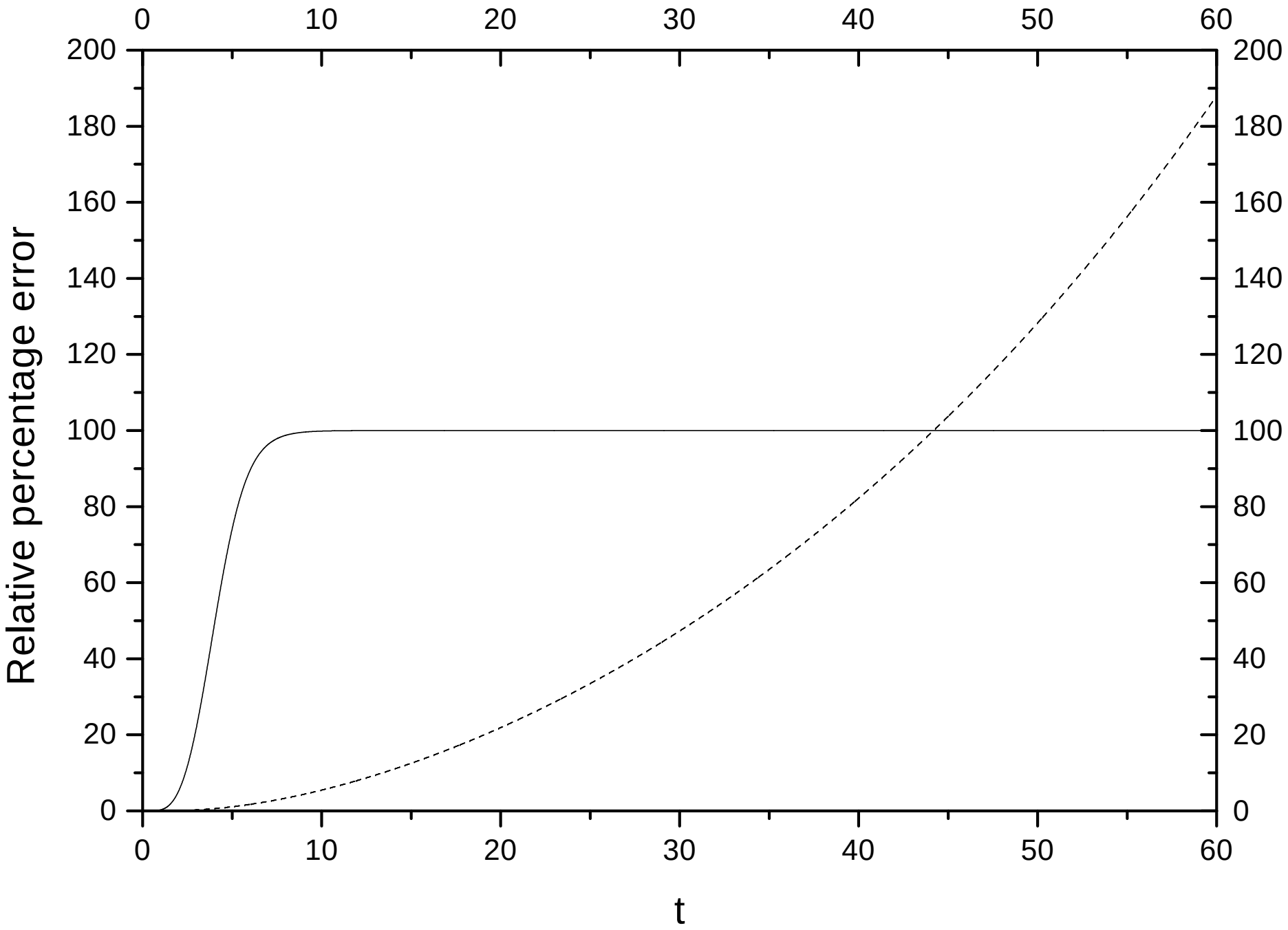
Relative percentage error
t
0
10
20
30
40
50
60
0
20
40
60
80
100
120
140
160
180
200

Fig. 17

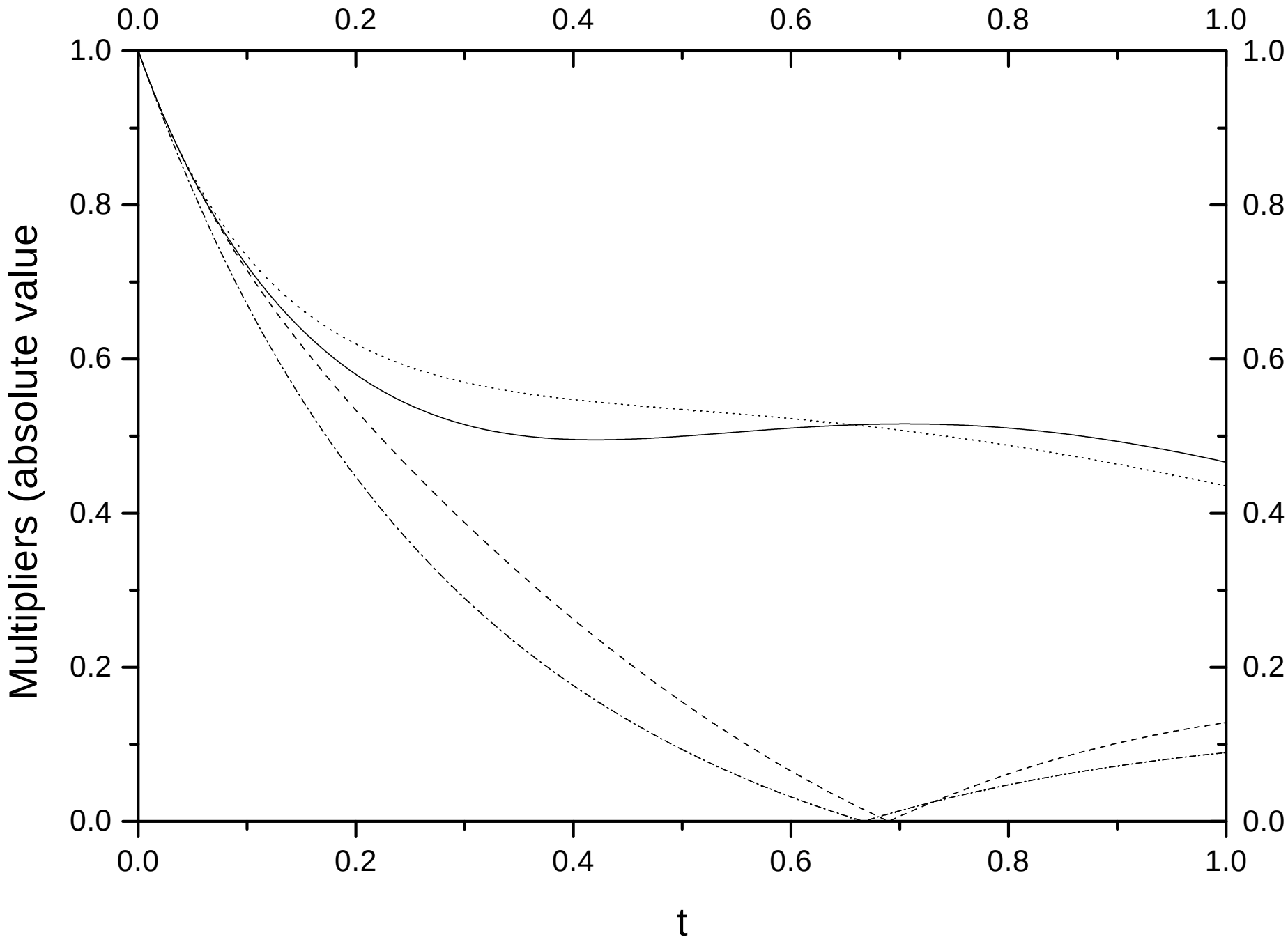

Fig. 18

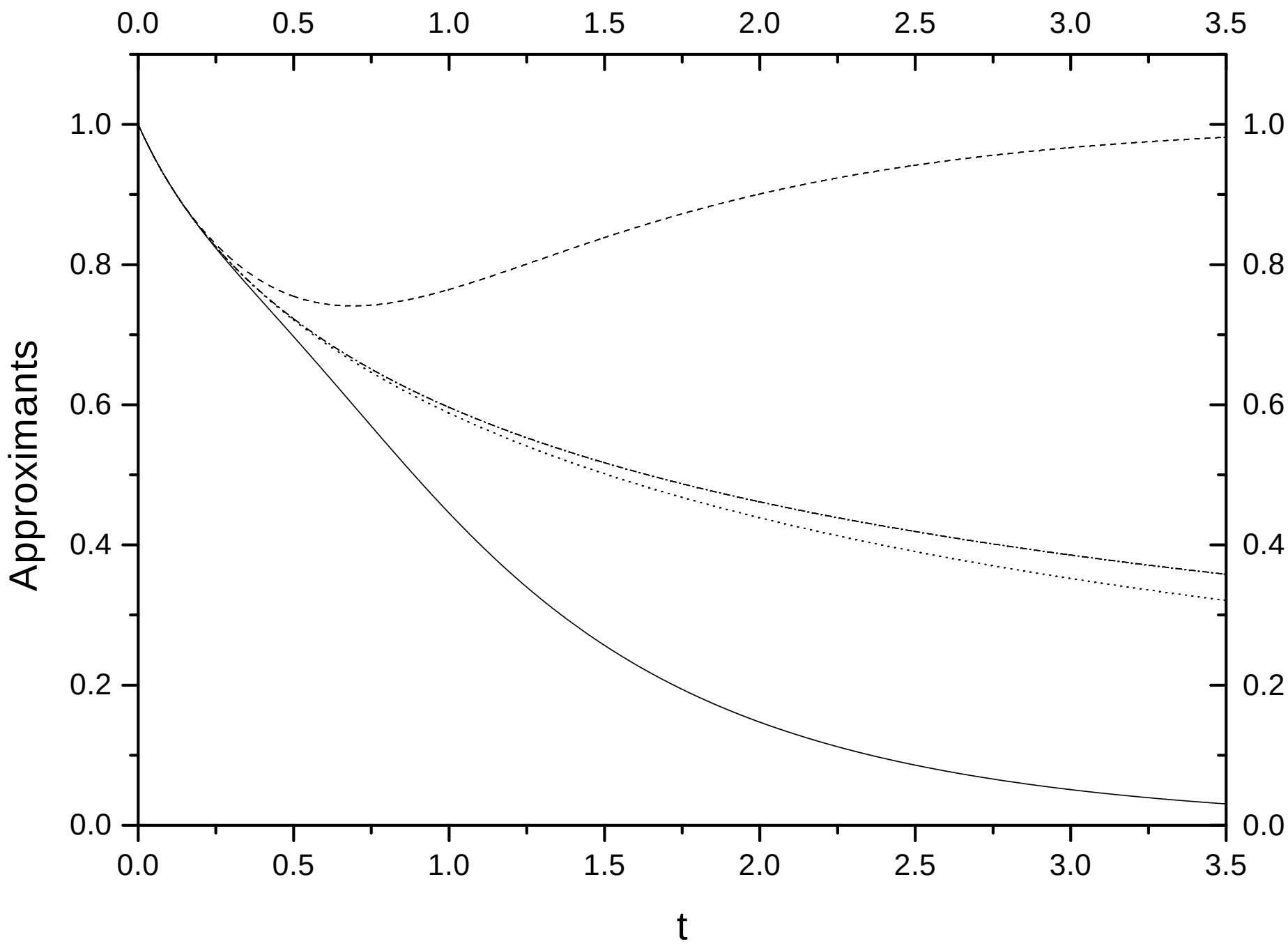

Fig. 19

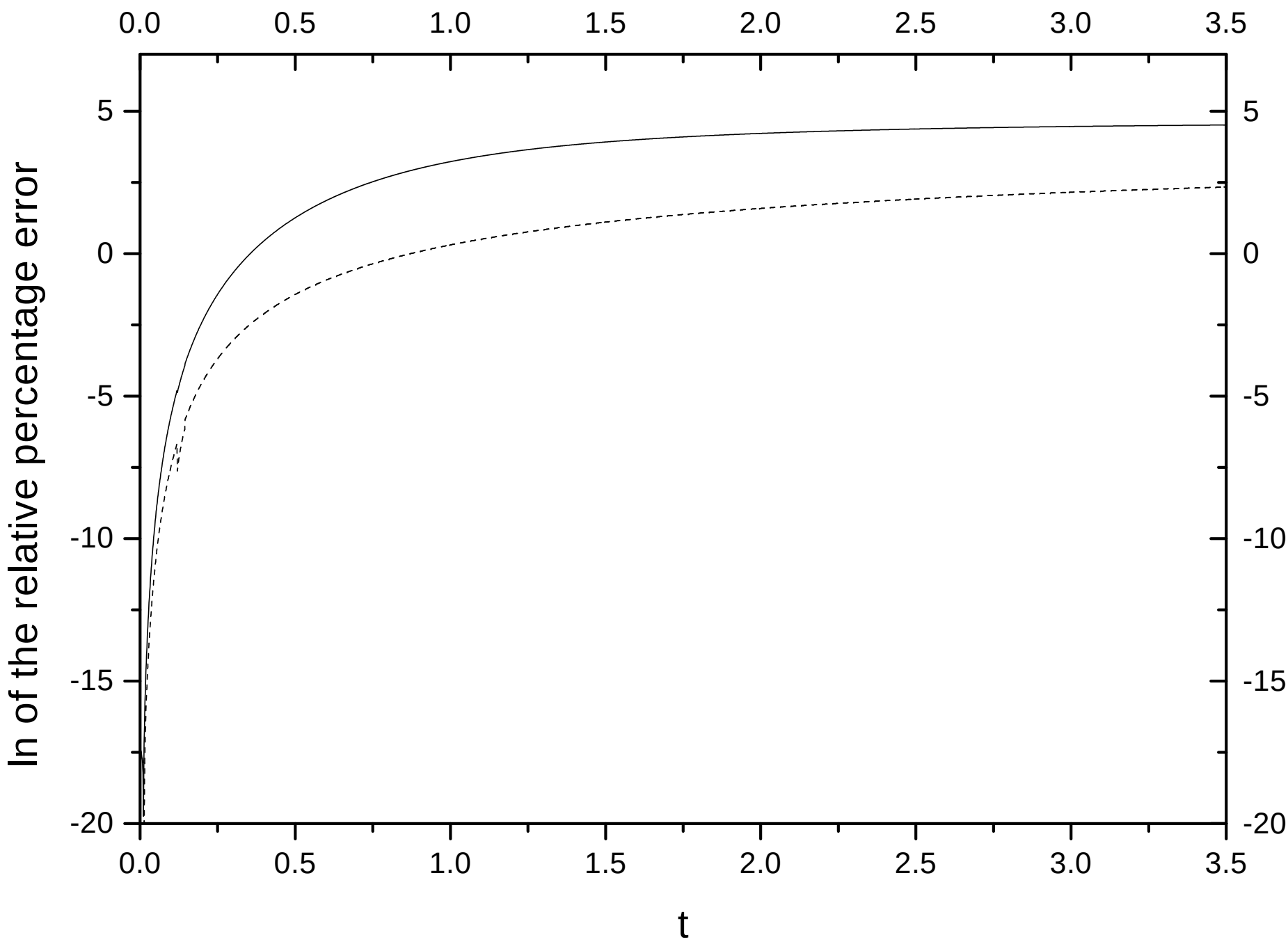
0.0
0.5
1.0
1.5
2.0
2.5
3.0
3.5
5
0
-5
-10
-15
-20
ln of the relative percentage error
t

Fig. 20

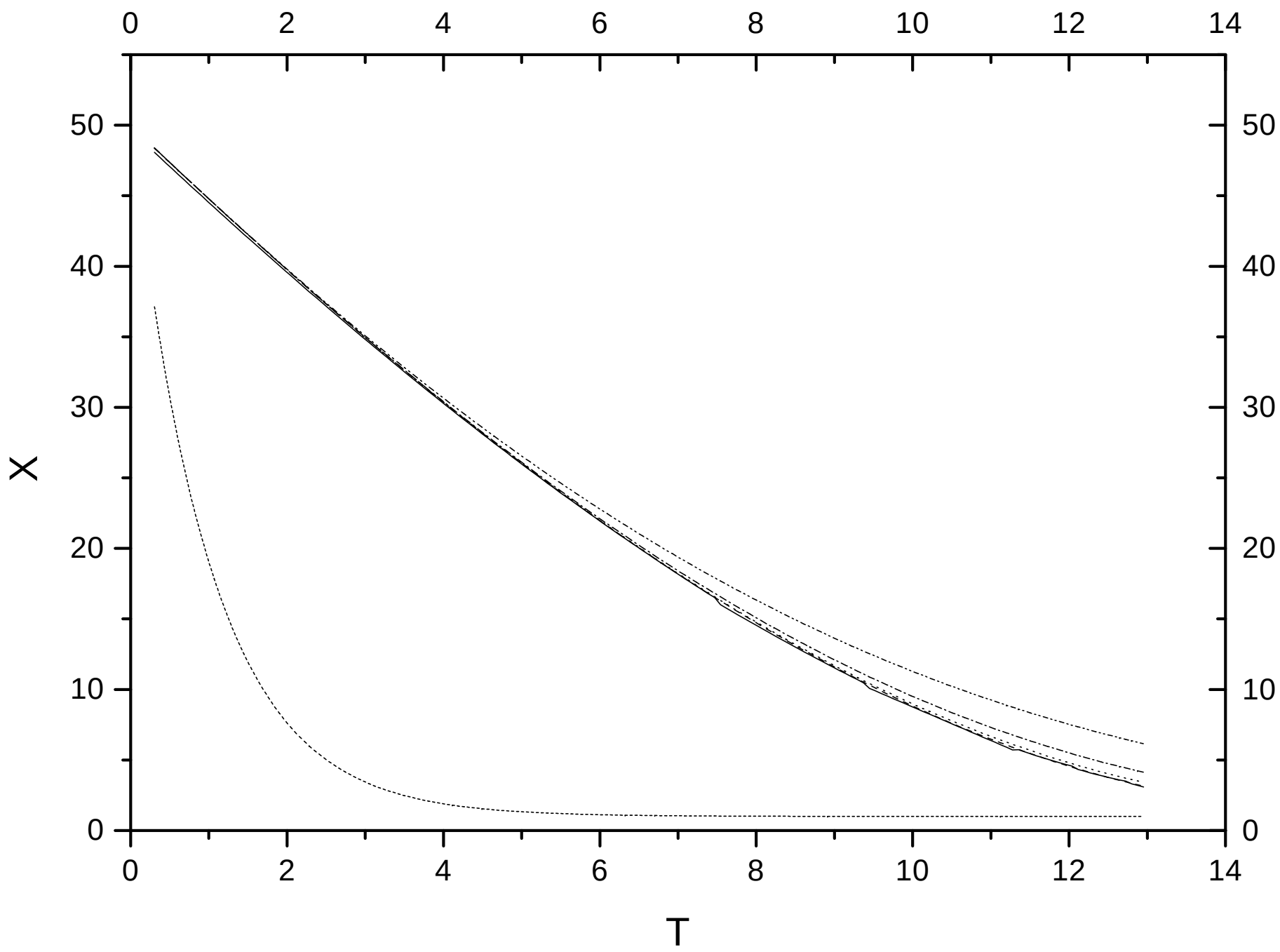

Fig. 21